GEOPHYSICAL EXPLORATION IN MARIE BYRD LAND, ANTARCTICA

CHARLES R. BENTLEY AND FENG-KENG CHANG

Geophysical and Polar Research Center, Department of Geology, University of Wisconsin, Madison 53705

Seismic, gravimetric, altimetric, and magnetic observations made along oversnow traverses in Marie Byrd Land and vicinity in 1959 and 1960 have provided a reconnaissance picture of this part of West Antarctica. The ice sheet surface slopes gently from a high in the region of the Executive Committee Range southwestward to the Ross ice shelf, but elsewhere exhibits a more complicated topography affected by the rugged subglacial relief. Before the formation of the ice sheet, a large island probably extended unbroken from the volcanic Executive Committee Range or Crary Mountains in the east to Edward VII Peninsula in the west, bounded on the north by open ocean and on the south by the Byrd subglacial basin. Lying off the east and northeast coast were several smaller volcanic islands. The mountains in the north-central part of this main island appear to belong to the plutonic and metamorphic province to the west. Throughout most of the region, there appears to be isostatic compensation for both the ice and the subglacial topography. Negative isostatic anomalies of −30 to −40 mgal occur near the Amundsen Sea coast, and associated with, but not superimposed upon, a subglacial trough in western Marie Byrd Land.

According to the description published before the International Geophysical Year by the *U.S. Board on Geographic Names* [1956], Marie Byrd Land is 'that portion of Antarctica lying east of Ross Ice Shelf and Ross Sea and south of the Pacific Ocean, extending approximately eastward to a line between the head of Ross Ice Shelf and Eights Coast' (about 100°W). However, 'the eastern limit of this land has been arbitrarily adopted, pending more definite mapping which may make it possible to draw boundaries along lines of natural demarcation.' No southern limit is given, since the interior of West Antarctica was nearly unknown at the time.

From geophysical observations on oversnow traverses conducted during and after the IGY, we now know that beneath a large part of the West Antarctic ice sheet the rock floor lies far below sea level. This region, which would be water-covered if the ice sheet were to melt (even after making allowance for isostatic rebound), has been named the Byrd subglacial basin. It runs from the Ross Sea south of the mountains of Marie Byrd Land as far as 100°W; eastward of this longitude it apparently forms a broad connection to the Amundsen Sea, as well as extending nearly to the Bellingshausen Sea [*Bentley,* 1964]. Even though it is not perfectly defined, the basin thus provides a natural subglacial boundary for Marie Byrd Land. We propose, then, that Marie Byrd Land be defined to be that part of Antarctica lying between the Ross Sea on the west, the Pacific Ocean on the north, and the Byrd subglacial basin on the south and east (see Figure 12). It is in this sense that the name will be used in the text of this paper. Maps, although labeled Marie Byrd Land, extend beyond its boundaries.

During 1959 and 1960, traverse parties carried out a reconnaissance examination of Marie Byrd Land. The major traverse was conducted during the 1959–1960 field season, the program including seismic reflection and refraction shooting, gravimetric and magnetic observations, and measurements of surface elevation. The traverse party left Byrd station on November 5, 1959, proceeding to the edge of the ice shelf bordering the Amundsen Sea at 73°55′S, 116°11′W via the Crary Mountains and Toney Mountain (Figure 2; see Figure 1 for index map). The same route was followed back as far as Toney Mountain (station 288 on the northward journey and station 493 returning), and re-measurements were made at all gravity, magnetic, and elevation stations. From there, the trail party traveled westward past the Usas Escarpment, Mount Petras, and the Flood Range to the Clark Mountains, thence southwestward to the Army-Navy Drive and back along this trail to Byrd station. The party reached Byrd station on February 8, 1960, after traveling a little more than 2000 km (about 1100 n. mi.).

In the preceding March, an 840-km (450-n. mi.)

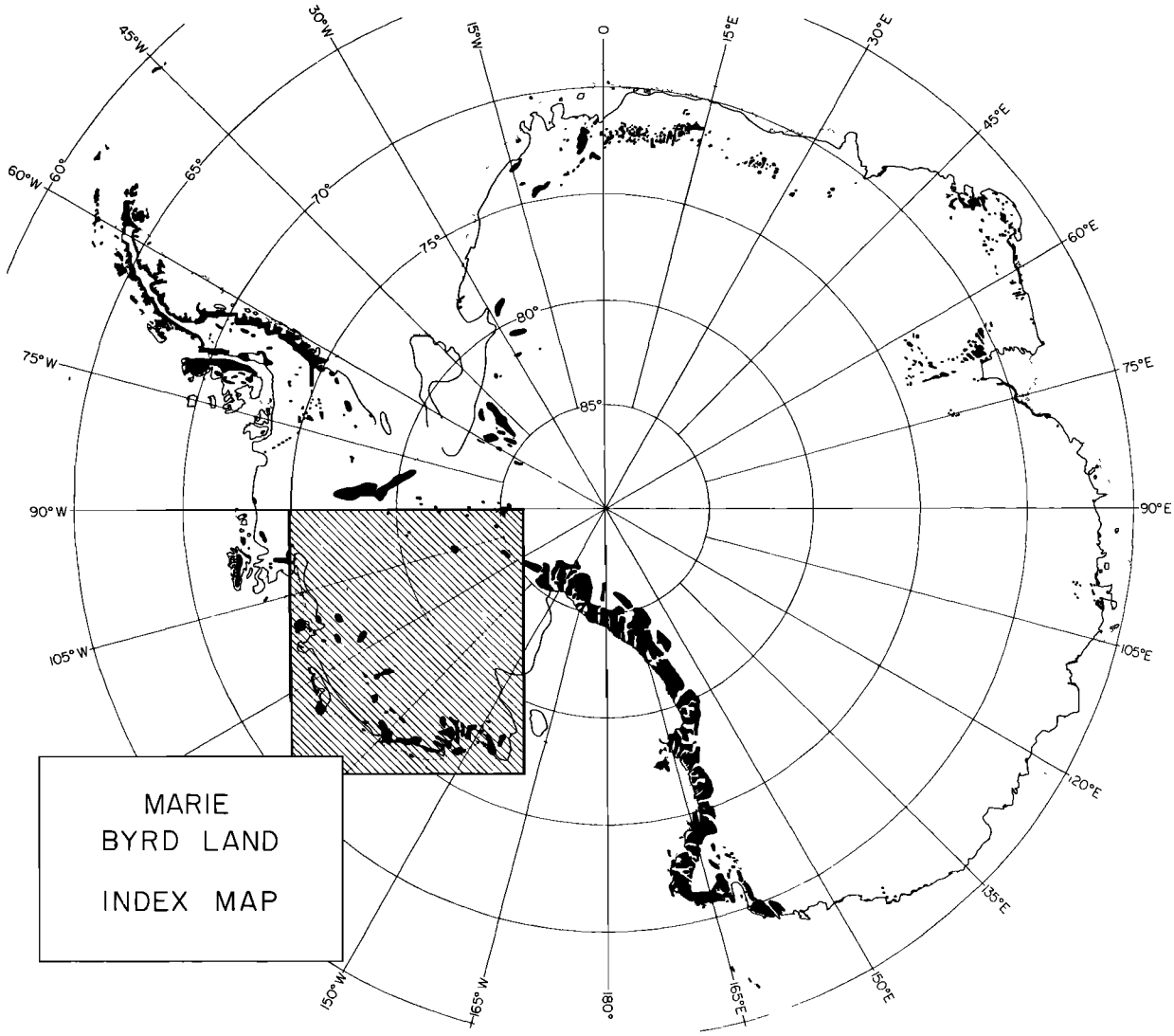

Fig. 1. Index map of Antarctica showing location of Marie Byrd Land.

trip along a triangular route was made to examine the geology of the Executive Committee Range and to cache fuel for the traverse the next summer. Surface elevation measurements were made, but time limitations and failure of equipment prevented other geophysical observations.

Included in this paper are the results of seismic soundings and elevation measurements made on the final section of the 1958–1959 Horlick Mountains traverse, from 82°08′S, 109°14′W to Byrd station, since the preceding report [*Bentley and Ostenso*, 1961] covered only observations up until the departure of the IGY party from the field on January 8, 1959. Magnetic data that were also collected have not yet been analyzed.

Members of the field party for the last part of the Horlick Mountains traverse were W. Chapman (leader), Chang, H. LeVaux, G. A. Doumani, and G. Bennett; for the Executive Committee Range traverse, J. Pirrit (leader), Chapman, Doumani, and Bennett; and for the Marie Byrd Land traverse, Pirrit (leader), Chang, P. E. Parks, LeVaux, Chapman, Doumani, Bennett, E. Boudette, K. Marks, and G. Widich.

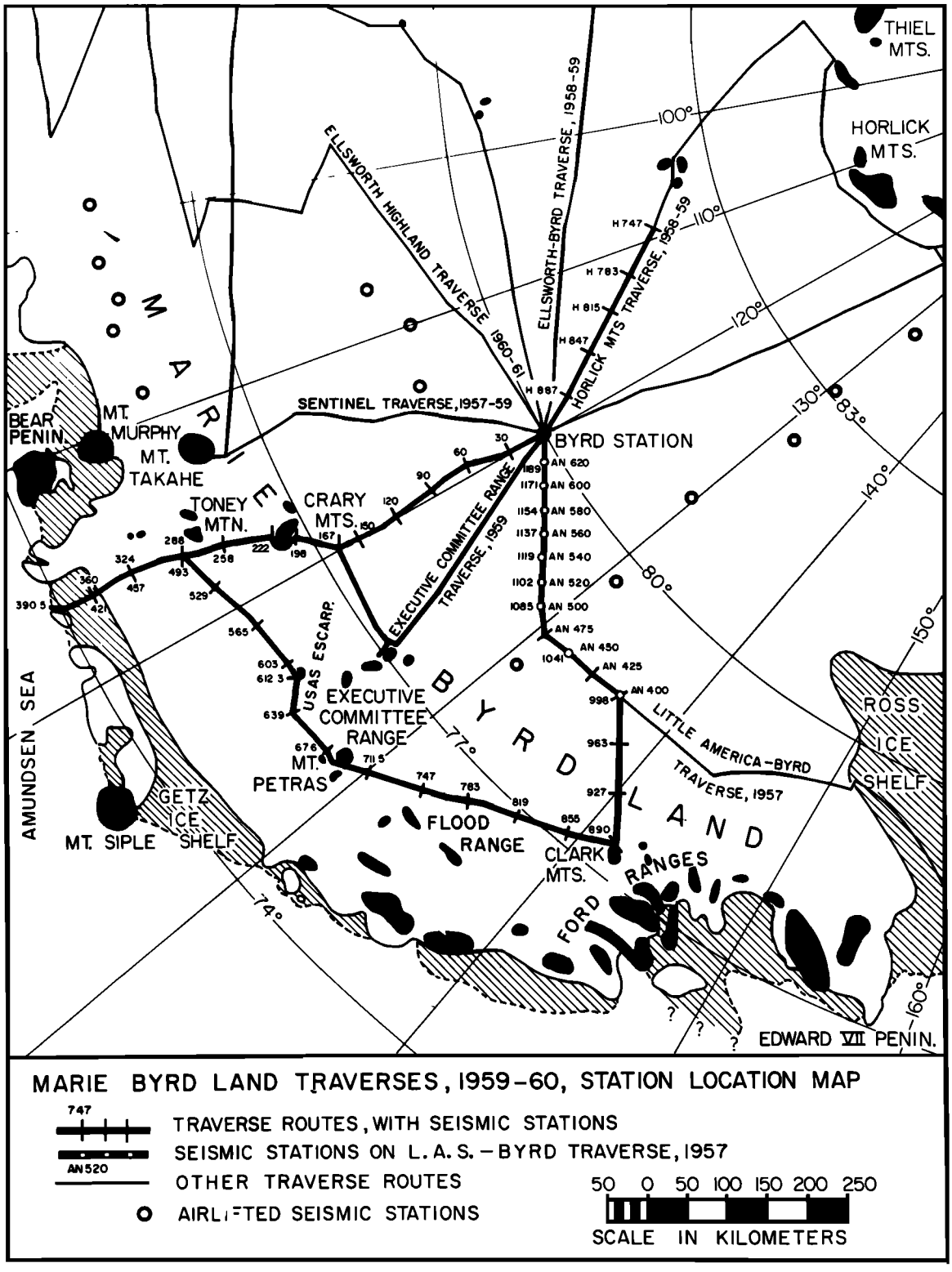

Fig. 2. Oversnow traverse routes in Marie Byrd Land.

GEOLOGIC SETTING

Discussions of the geological findings of these traverses have already been published [*Doumani and Ehlers,* 1962; *Doumani,* 1964]. The Executive Committee Range comprises five volcanic cones. Only two were visited, but according to their appearance from the air the others should be similar in nature. The rocks are exclusively basic volcanics, including basalts, andesites, and trachytes. Similar rocks are found in the Crary Mountains, which comprise four peaks, one about 25 km southeast of the other three, on Toney Mountain, which consists of two peaks about 20 km apart, and on Mount Takahe, 70 km to the east [*Anderson,* 1960]. The Usas escarpment and Mount Petras, which lie north of the Executive Committee Range, are composed, on the other hand, of rhyolitic and dacitic tuffs and flows, with relatively small amounts of granodiorite and basalt. Farther to the west, the Clark Mountains contain granodiorite, granite, and unfolded metasedimentary rocks that dip gently to the southeast. Still farther west in the Ford Ranges, beyond the limit of the traverse, highly folded geosynclinal sediments intruded by a suite of acidic batholiths were already known [*Warner,* 1945; *Passel,* 1945]; to the north in the same range, in the Fosdick Mountains, volcanic rocks are again found [*Fenner,* 1938]. The Rockefeller Mountains, in the western extremity of Marie Byrd Land, are composed of granite and metasediments [*Wade,* 1945].

FIELD EQUIPMENT AND PROCEDURES

The operating procedures in the field were similar to those of previous traverses [*Bentley and Ostenso,* 1961]. Standard seismic stations were spaced at intervals of 55 to 67 km (30 to 36 n. mi.). Besides reflection sounding, observations at seismic stations included snow-pit studies, determinations of temperature in 10-meter boreholes, gravimetric and magnetic measurements, solar observations to determine station position, and azimuth measurements on mountain peaks. Intermediate stations were made about every 5½ km (3 n. mi.), where altimetric, magnetic, gravimetric, and rammsonde data and measurements of wind speed, wind direction, and air temperature were recorded.

These procedures were followed on the Marie Byrd Land traverse up to the junction with the Army-Navy Drive. From this point on, soundings were made only at stations AN425 and AN475, where seismic measurements had not been made by the Little America–Byrd traverse party [*Bentley and Ostenso,* 1961], and gravity, magnetic, and elevation measurements were made at the stations 8 km apart that had been occupied by the earlier group. On the last part of the Horlick Mountains traverse, the standard procedures were followed, except that gravity observations were not made, since the gravimeter was not in operation.

For the seismic work, a 24-trace Texas Instruments 7000B Portable Seismograph System was used. This unit has a basic frequency range of 5 to 500 Hz and a wide range of possible filter settings. Automatic gain control and mixing are also provided, but were not generally used, as experience had shown that neither produced significant improvement in the quality of the seismograms. Furthermore, it was desirable to record true amplitudes of ground motion. Power was provided by two 12-volt heavy-duty lead-acid batteries that were charged from the vehicle generator system.

The seismic spreads normally comprised two cables, each with 12 geophones at 30-meter intervals. Three of the geophones on each cable were often placed horizontally to detect possible shear or transformed compressional-shear reflections. The cables were laid out either in line, with shots fired in the center, or in the form of an L, with shots at the corner. The charge usually consisted of a one-pound Nitramon primer or a primer with one or two pounds of Nitramon S fired in a three- or four-meter auger hole. Low-cut filtering was usually set at 60 or 90 Hz, and high-cut at 160 or 215 Hz. Failure to record a reflection occurred only at station 30 early in November, when the shot-generated noise level was still high, and at station 603, where the ice was thin. At other stations, the reflection quality was generally excellent (Figure 3).

Frost gravimeter C2-55, a temperature-controlled meter with low drift characteristics, was used for the gravity measurements on the Marie Byrd Land traverse. With a calibration constant of 0.08213 mgal/scale division, this meter had a reading range without resetting of only 125 mgal.

Before the start of the traverse, in the expectation of low ambient temperatures in the traverse vehicle, the operating temperature of the gravimeter was set to 68°F (20°C), some 50°F (28°C) below its ordinary operating temperature. This proved to be a mistake, since the temperature inside the vehicle frequently exceeded 68°F (20°C). As a result, tem-

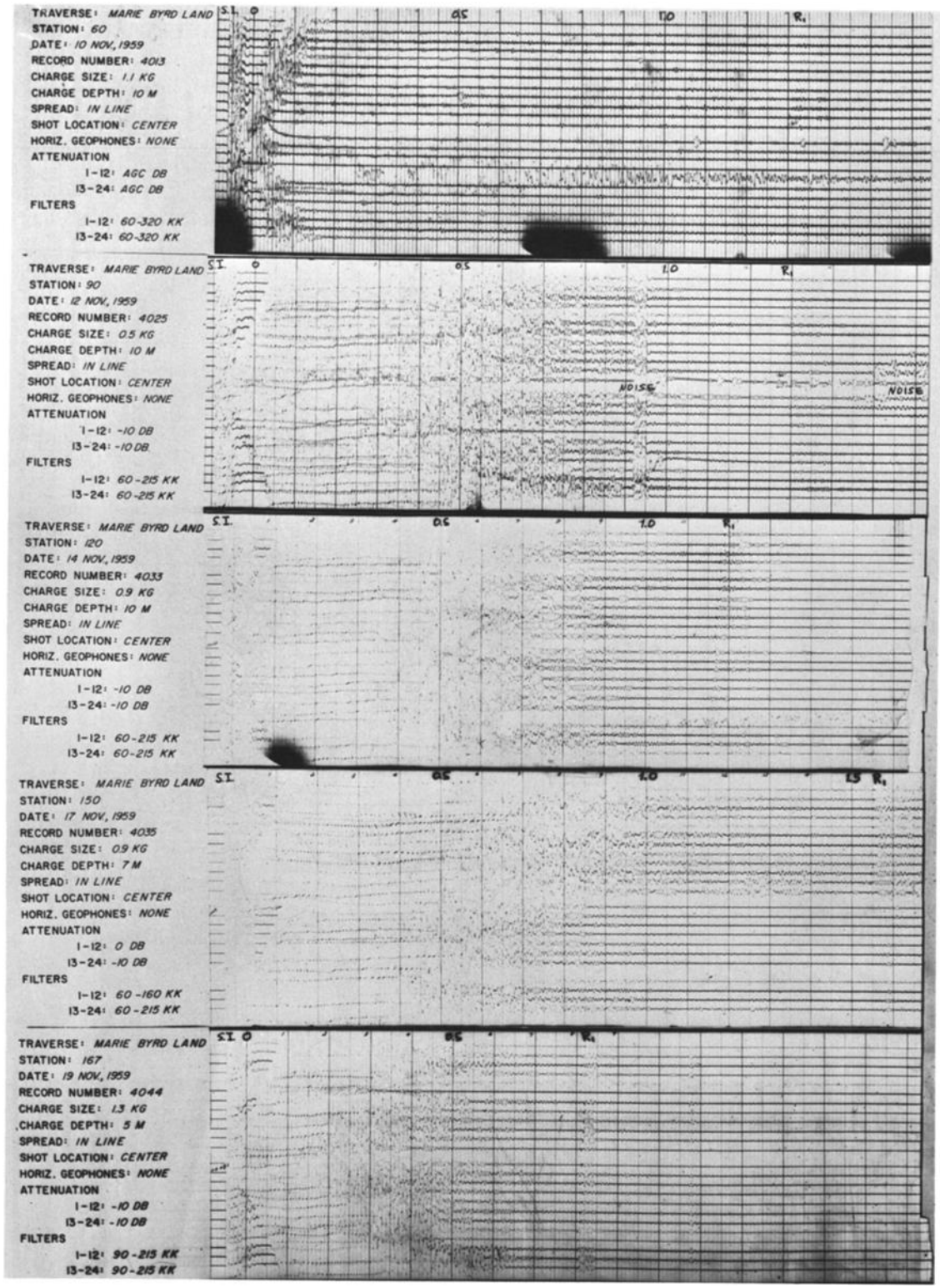

Fig. 3. Seismograms. Heavy timing lines 0.1 sec apart. *S.I.*: shot instant. R_1: reflection from ice-rock interface. R_{1P}, R_{1S}, R_{PS}: P, S, and converted P to S (and S to P) reflections from ice-water interface, respectively. R_W: reflections from water-sediment interface. R_1': reflection from sediment-rock interface. R_2: first multiple from ice-rock interface. (Continued on following pages.)

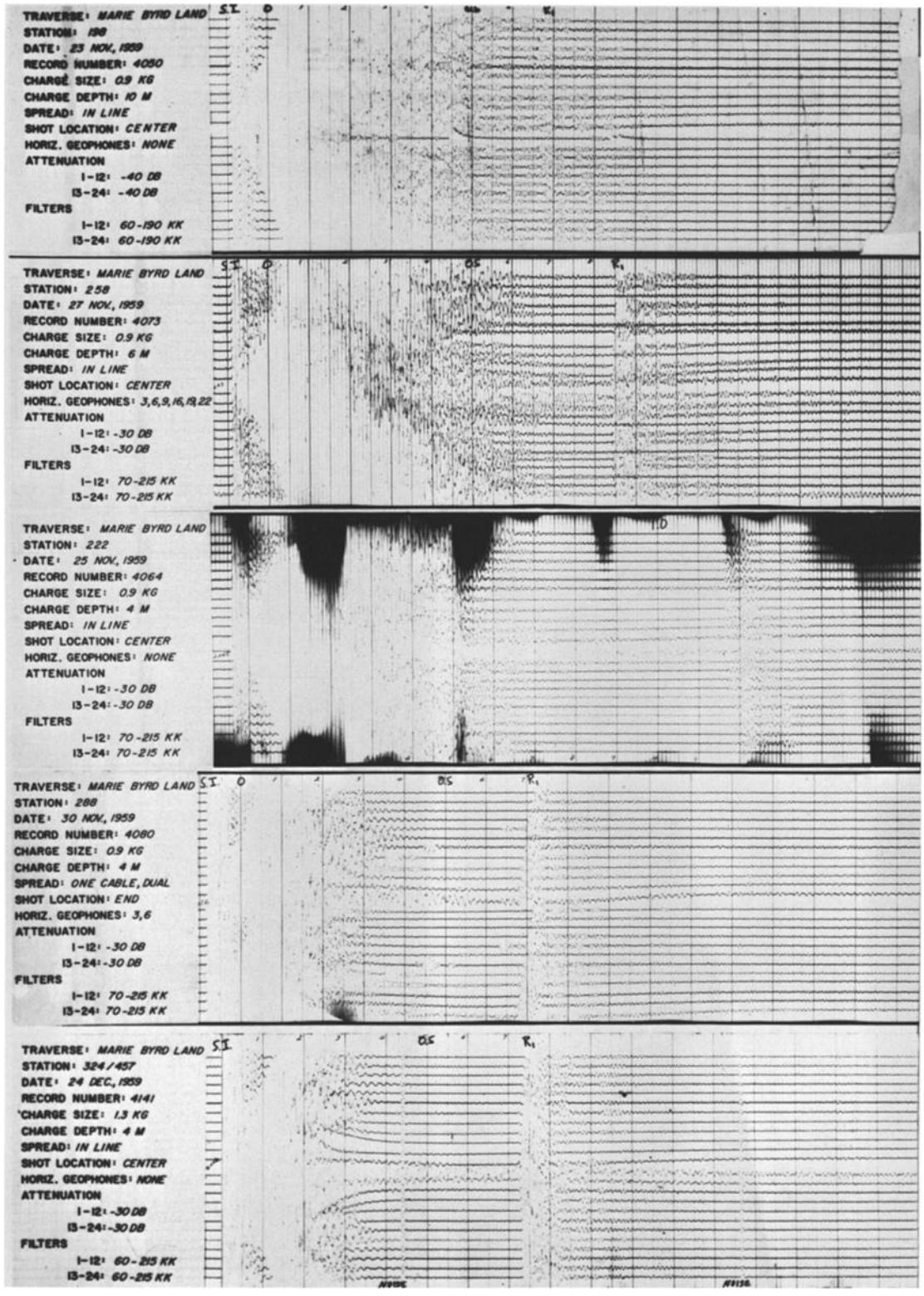

Fig. 3. (continued)

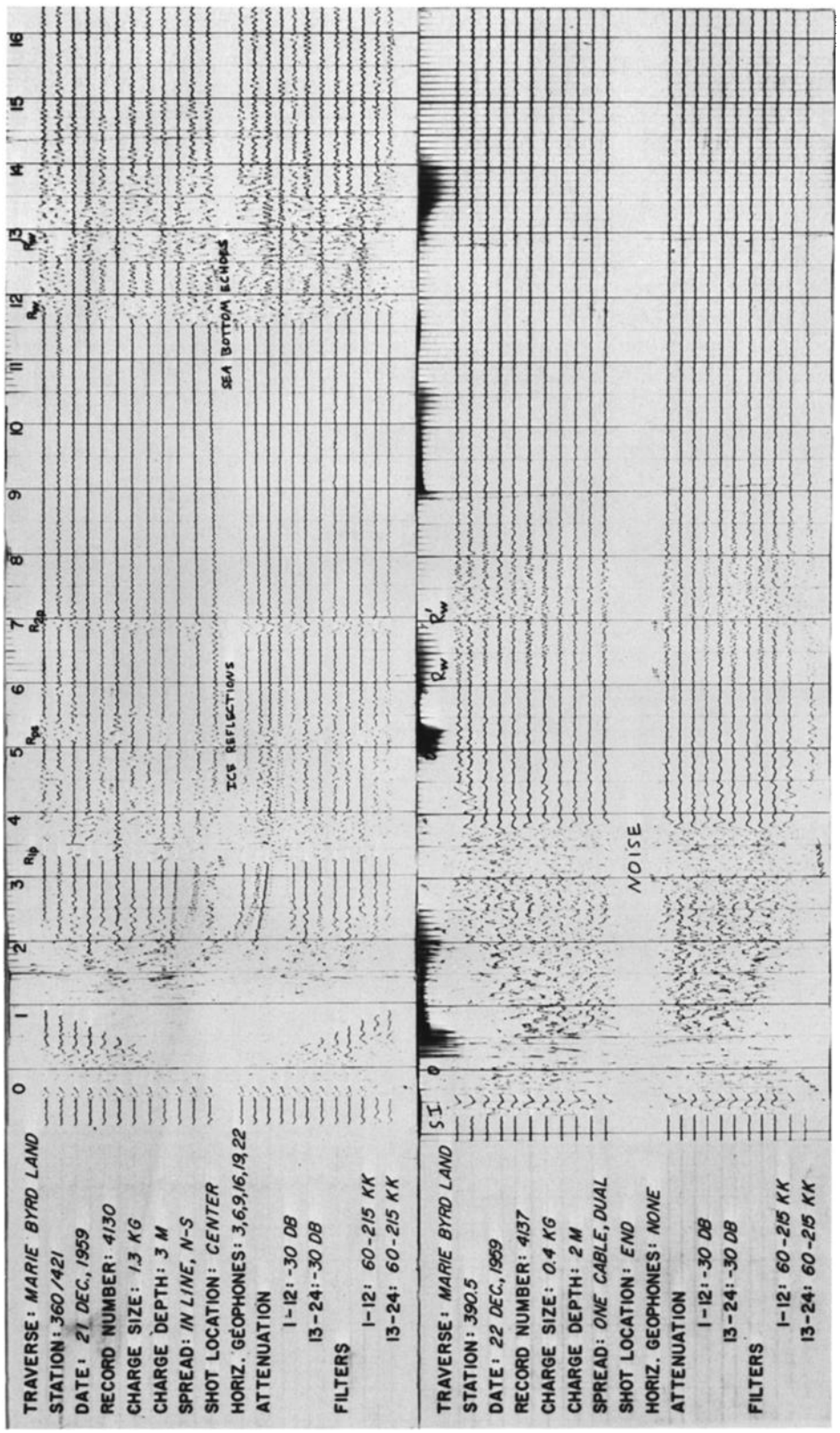

Fig. 3. (continued)

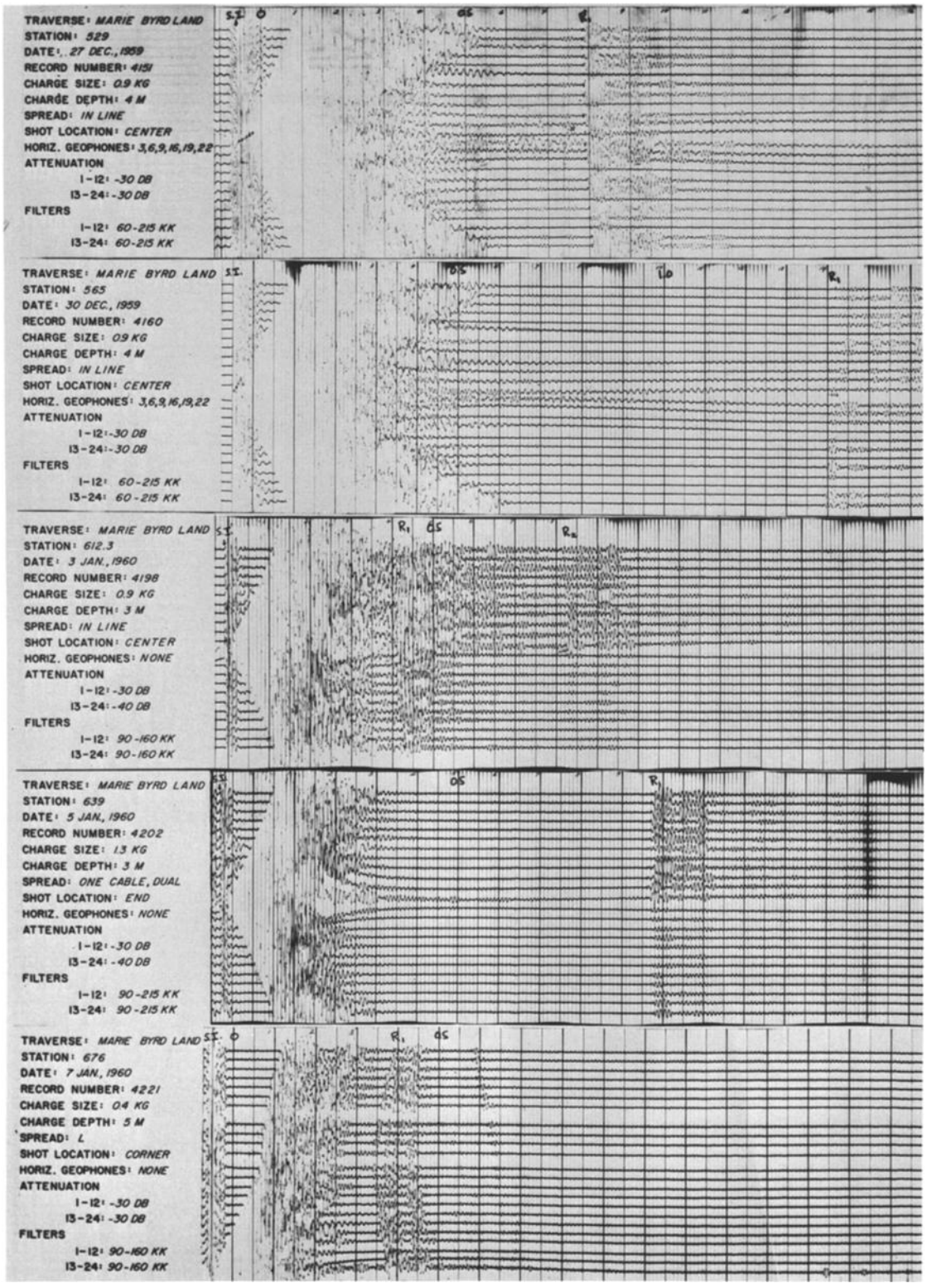

Fig. 3. (continued)

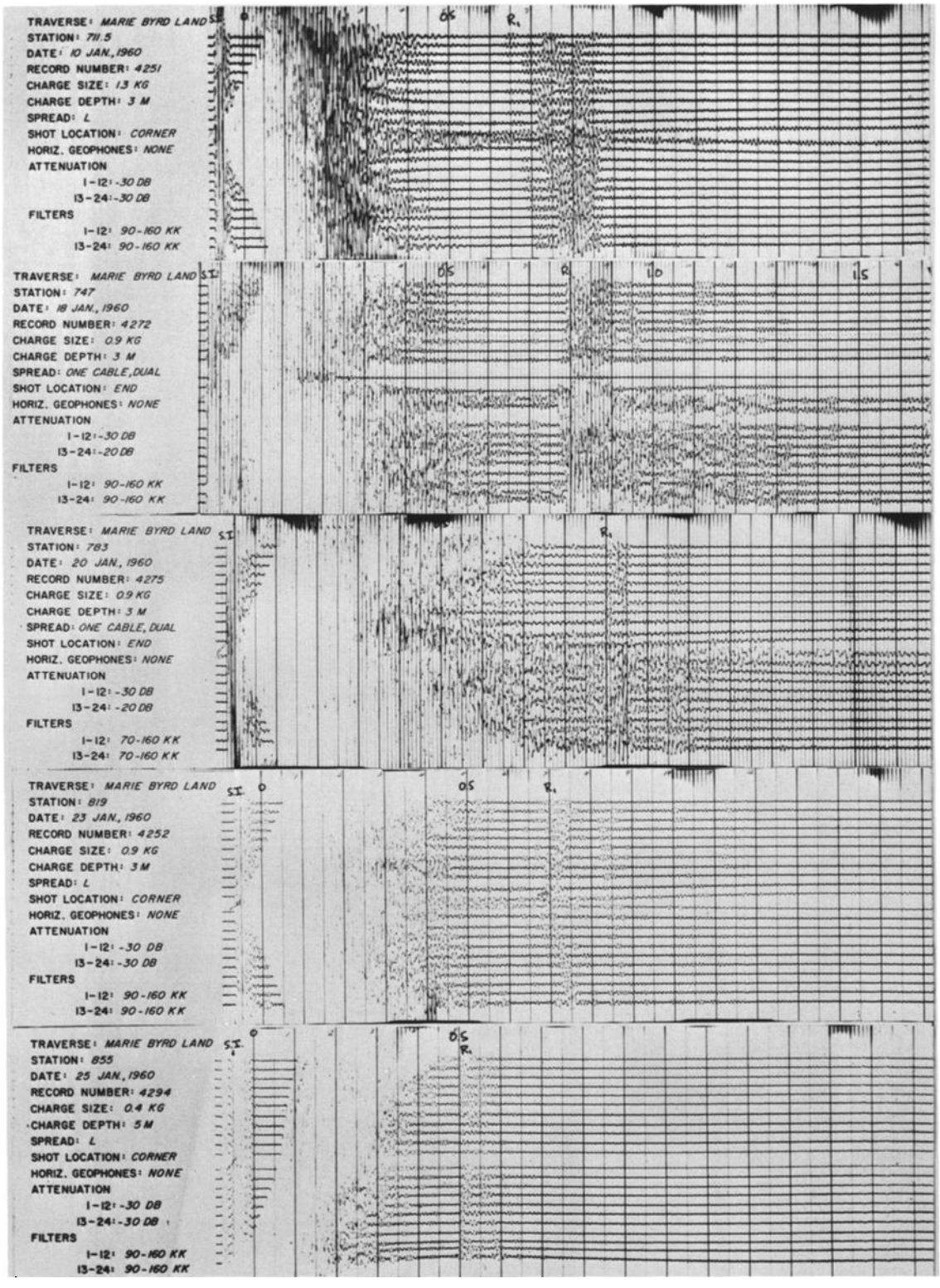

Fig. 3. (continued)

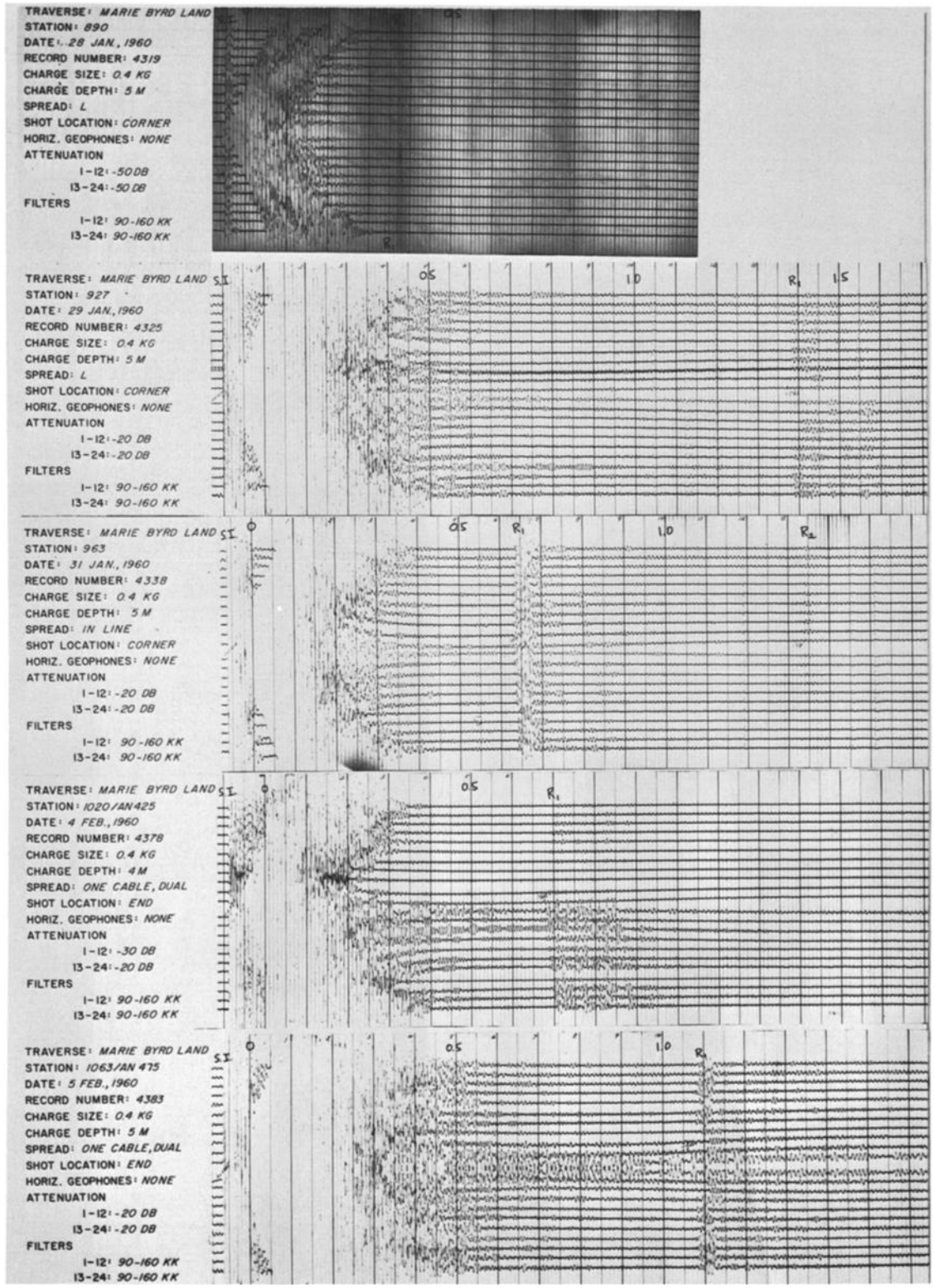

Fig. 3. (continued)

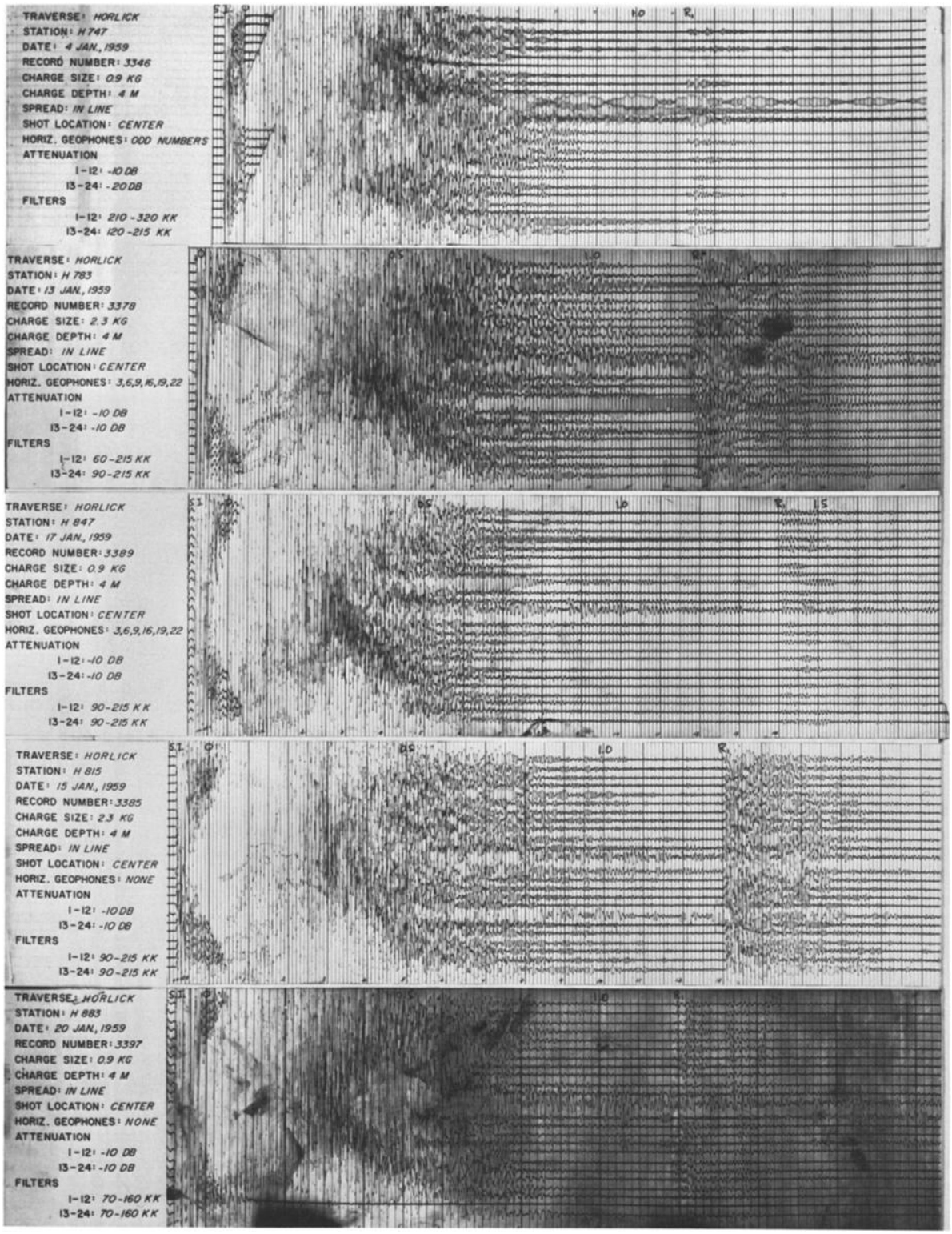

Fig. 3. (concluded)

perature regulation was lost. Rather than attempting to change the operating temperature under difficult field conditions and with time at a premium, a record of meter temperature was kept, and corrections to the observed gravity values were applied as described below.

An Arvela vertical-component magnetometer, model T7, was used for magnetic measurements. This is a wide-range null-reading instrument with temperature compensation. Two magnetic observations were made at each station, one with the magnetometer oriented toward magnetic north and the other with it oriented toward the south, in order to eliminate the effect of imperfect level of the instrument, as well as to obtain an estimate of the reading error. The calibration constant of the instrument, as determined before the traverse, was 27.3 γ/scale division. The magnetometer suffered a bad jar between stations 526 and 529, incurring a tare of about 500 γ, although there was no apparent damage to the instrument. Unfortunately, the calibration constant was not checked immediately after this accident, but at the termination of the traverse it had changed only 1% to 27.6 γ/scale division.

Elevations were measured with four Wallace and Tiernan altimeters (until one broke; see below). The altimeters were carried in two traverse vehicles traveling 5.5 km (3 n. mi.) apart, the rear vehicle occupying successive stations previously occupied by the lead vehicle. Readings were coordinated by radio. Wind speed, wind direction, and temperature measurements were taken at each station. All altimeters were read together at the beginning and end of each travel day.

Station positions (Table 1) were determined from sun lines at seismic stations and by dead reckoning at intermediate points. The observations were made by W. H. Chapman of the U.S. Geological Survey.

DATA REDUCTION

Altimetry

The altimetric data were reduced in the following way. Differences between readings of two separate pairs of altimeters at consecutive stations on the Marie Byrd Land traverse (corrected for the atmospheric temperature) were computed and averaged up to station 606, where one altimeter ceased to operate. From there on, only one set of differences was computed, the third altimeter being used as a check against reading errors. Instrument temperature corrections were applied to the indicated elevations. The index correction for altimeter pairs was calculated from the differences in indicated elevation when altimeters were read together at the beginning and end of each travel day. Any change in this index correction was distributed linearly through the day. On the Executive Committee Range traverse, only three altimeters were used, and the reduction method was the same as for the latter part of the Marie Byrd Land traverse.

Elevations determined on the two traverses along their common section of track were averaged from Byrd station to station 75, the Marie Byrd Land traverse values being used from there on. For the repeated traverse section between Toney Mountain and the Amundsen Sea coast, the values from the return journey were used, since wind measurements indicated more stable pressure conditions. Along the Army-Navy Drive, elevations computed from the two traverses were averaged.

Pressure corrections were applied according to the synoptic 700-mbar pressure maps for the Antarctic regions prepared at the International Antarctic Analysis Centre in Melbourne. The accumulated correction increased gradually from Byrd station to the Amundsen Sea, where it reached a value of +50 meters. From there it decreased slowly to a minimum value of −25 meters near the junction with the Army-Navy Drive, and returned nearly to zero upon return to Byrd station. Closure corrections of +10 meters at the Amundsen Sea (where absolute elevation was determined from optical angles measured to an iceberg) and −20 meters at Byrd station were distributed linearly along the corresponding sections of the traverse. Corrected elevation values are listed in Table 1.

The error in elevation determinations is difficult to estimate. The root-mean-square difference between values computed on the two traverses along the Army-Navy Drive was about 12 meters; between values computed along the Marie Byrd Land traverse and the Executive Committee Range traverse, about 25 meters; between those on the outgoing and return legs to the Amundsen Sea coast, about 20 meters. Other clues to elevation accuracy are provided by the closure errors and the magnitude of the pressure corrections. Because several checks were available in the course of the traverse, we estimate the error to be about ±25 meters relative to Byrd station, a value somewhat better than the average for Antarctic traverses [*Bentley*, 1964].

TABLE 1*a*. Station Positions and Elevations, Gravity and Seismic Results, Marie Byrd Land Traverse

Station	South Latitude	West Longitude	Surface Elevation (meters a.s.l.)	Observed Gravity (gals)	Free Air Anomaly (milligals)	Bouguer Anomaly (milligals)	Seismic Reflection Time[a] (seconds)	Shot Depth (meters)	Ice Thickness (meters)	Rock Elevation (meters a.s.l.)
0(Byrd)	79°59.2'	120°01.0'	1525	982.5960	+ 2.4				2645 b	-1120 b
3	79°56.3'	120°00.0'	1522	982.5828	- 9.7				2802	-1280
6	79°53.3'	120°00.0'	1518	982.5875	- 6.3				2725	-1207
9	79°50.3'	120°00.0'	1519	982.5754	-15.4				2841	-1322
12	79°47.3'	120°00.0'	1525	982.5795	- 7.9				2217	-1187
15	79°44.3'	120°00.0'	1535	982.5702	-12.5				2271	-1232
18	79°41.5'	120°00.0'	1543	982.5752	- 3.6				2094	-1076
21	79°38.6'	120°02.0'	1549	982.5684	- 7.0				2129	-1106
24	79°35.7'	120°02.0'	1547	982.5646	- 9.8				2171	-1126
27	79°32.8'	120°02.0'	1542	982.5556	-18.8				2900	-1238
*30	79°29.7'	120°02.0'	1538	982.5538	-20.2		N.R.		2706	-1238
33	79°26.8'	119°59.0'	1537	982.5562	-16.6				2671	-1163
36	79°23.8'	119°55.0'	1546	982.5576	-10.7				2085	-1052
39	79°20.9'	119°52.0'	1556	982.5559	- 7.7				2108	- 985
42	79°18.0'	119°49.0'	1564	982.5444	-15.1				2122	-1074
45	79°15.0'	119°46.0'	1569	982.5385	-17.9				2665	-1096
48	79°12.0'	119°44.0'	1571	982.5325	-21.6				2701	-1130
51	79°09.0'	119°42.0'	1581	982.5321	-17.2				2623	-1042
54	79°06.0'	119°40.0'	1581	982.5298	-17.9				2611	-1030
57	79°03.1'	119°37.0'	1586	982.5282	-16.3				2570	- 984
*60	79°00.2'	119°34.0'	1592	982.5234	-17.6	- 7.7	1.357	10	2573 b	- 981 b
63	78°57.4'	119°36.0'	1597	982.5242	-13.7				2530	- 933
66	78°54.3'	119°38.0'	1581	982.5271	-14.0				2530	- 949
69	78°51.1'	119°39.0'	1596	982.5148	-19.8				2642	-1046
72	78°48.3'	119°40.0'	1601	982.5204	-11.0				2526	- 925
75	78°45.3'	119°41.0'	1616	982.5269	+ 1.8				2360	- 744
78	78°42.4'	119°42.0'	1631	982.5218	+ 3.0				2369	- 738
81	78°39.4'	119°42.0'	1644	982.5026	-10.5				2595	- 951
84	78°36.3'	119°42.0'	1639	982.4967	-16.1				2690	-1051
87	78°33.3'	119°43.0'	1638	982.4993	-12.0				2633	- 995
*90	78°30.3'	119°43.0'	1655	982.4981	- 6.2-	- 3.0	1.358	10	2575 b	- 920 b
93	78°27.3'	119°45.0'	1657	982.5006	- 1.3				2505	- 848
96	78°24.3'	119°46.0'	1661	982.5027	+ 3.8				2435	- 774
99	78°21.2'	119°48.0'	1675	982.4953	+ 2.6				2468	- 793
102	78°18.1'	119°49.0'	1686	982.4875	+ 0.1				2519	- 833
105	78°15.1'	119°50.5'	1690	982.4798	- 5.5				2609	- 919
108	78°12.1'	119°53.0'	1706	982.4678	- 9.8				2691	- 985
111	78°09.0'	119°55.0'	1708	982.4695	- 5.7				2633	- 925
114	78°06.0'	119°58.0'	1715	982.4751	+ 3.9				2498	- 783
117	78°03.0'	120°00.0'	1721	982.4858	+18.3				2290	- 569
*120	77°59.8'	120°01.0'	1736	982.4827	+21.7	- 6.6	1.191	10	2256 b	- 520 b
123	77°56.8'	120°01.0'	1761	982.4748	+23.5				2266	- 505
126	77°53.8'	120°01.0'	1764	982.4808	+32.2				2151	- 387
129	77°50.8'	120°01.0'	1789	982.4567	+17.7				2406	- 617
132	77°47.8'	120°00.0'	1795	982.4368	+ 1.5				2667	- 872
135	77°44.8'	120°00.0'	1802	982.4244	- 6.9				2813	-1011
138	77°41.8'	120°00.0'	1800	982.4281	- 2.2				2752	- 952
141	77°38.8'	120°00.5'	1817	982.4502	+27.3				2339	- 522
144	77°35.9'	120°01.0'	1828	982.4469	+22.9				2428	- 600
147	77°32.9'	120°01.0'	1834	982.4214	+ 1.2				2772	- 938
*150	77°29.8'	120°01.0'	1832	982.4004	-12.1	+ 0.8	1.573	7	2983 b	-1151 b
153	77°27.0'	119°58.8'	1828	982.4104	- 1.5				2656	- 828
156	77°24.0'	119°57.5'	1858	982.4247	+24.0				2139	- 281
159	77°21.2'	119°55.4'	1872	982.4189	+24.3				1985	- 113
162	77°18.4'	119°52.5'	1879	982.4053	+14.7				1972	- 93
165	77°15.4'	119°52.0'	1891	982.4018	+16.8				1788	+ 103
*167	77°13.5'	119°51.0'	1884	982.4026	+16.7	- 74.3	0.860	6	1619 b	+ 265 b
171	77°10.2'	119°40.0'	1880	982.3818	- 3.1				1912	- 32
174	77°08.1'	119°30.5'	1860	982.3790	-10.7				2006	- 146
177	77°06.0'	119°20.5'	1855	982.3773	-12.8				2033	- 178
180	77°03.9'	119°11.3'	1814	982.3812	-20.0				2100	- 286
183	77°01.6'	119°01.5'	1809	982.3729	-28.3				2218	- 409
186	76°59.7'	118°51.5'	1808	982.3780	-22.4				2128	- 320
189	76°57.5'	118°42.2'	1803	982.3746	-25.8				2175	- 372
192	76°55.3'	118°33.2'	1800	982.3902	- 9.6				1928	- 128
195	76°53.3'	118°23.2'	1813	982.3900	- 4.5				1865	- 52
*198	76°51.0'	118°14.0'	1839	982.4117	+26.7	- 74.0	0.755	10	1423 b	+ 416 b
201	76°48.1'	118°20.0'	1882	982.4037	+34.0				1380	+ 502
204	76°44.9'	118°24.0'	1894	982.3870	+26.7				1524	+ 370
207	76°41.8'	118°22.4'	1909	982.4273	+70.1				912	+ 997
210	76°38.6'	118°22.5'	1805	982.4628	+75.7				747	+1058
213	76°36.1'	118°15.9'	1667	982.4420	+14.1				1557	+ 110
216	76°35.6'	118°02.5'	1625	982.4434	+ 2.9				1706	- 81

TABLE 1*a*. (continued)

Station	South Latitude	West Longitude	Surface Elevation (meters a.s.l.)	Observed Gravity (gals)	Free Air Anomaly (milligals)	Bouguer Anomaly (milligals)	Seismic Reflection Time[a] (seconds)	Shot Depth (meters)	Ice Thickness (meters)	Rock Elevation (meters a.s.l.)
219	76°36.4'	117°50.0'	1567	982.4457	-13.3				1913	- 346
*222	76°37.6'	117°37.0'	1559	982.4263	-35.9	- 44.2	1.201	4	2268 b	- 709 b
225	76°34.6'	117°34.0'	1554	982.4134	-48.3				2465	- 911
228	76°31.8'	117°30.2'	1562	982.3444	-113.0				3460	-1898
231	76°29.1'	117°26.9'	1561	982.3436	-112.3				3464	-1903
234	76°26.3'	117°23.6'	1561	982.3617	-92.3				3180	-1619
237	76°23.4'	117°20.5'	1554	982.4034	-51.8				2582	-1028
240	76°20.6'	117°17.5'	1544	982.4309	-24.0				2171	- 627
243	76°17.7'	117°14.0'	1542	982.4198	-34.1				2337	- 795
246	76°15.0'	117°10.0'	1547	982.4452	- 5.3				1926	- 379
249	76°12.1'	117°06.5'	1577	982.4659	+26.7				1492	+ 85
252	76°09.4'	117°03.7'	1587	982.4405	+ 6.2				1825	- 238
255	76°06.5'	117°00.3'	1586	982.4279	+ 5.4				1852	- 266
*258	76°03.7'	116°57.0'	1588	982.4433	+13.5	- 35.0	0.929	4	1749 b	- 161 b
261	76°00.7'	116°54.2'	1587	982.4211	- 7.0				1963	- 376
264	75°58.0'	116°51.0'	1589	982.4377	+12.2				1585	+ 4
267	75°51.9'	116°48.0'	1602	982.4455	+27.4				1277	+ 325
270	75°49.0'	116°47.1'	1612	982.4613	+49.3				866	+ 746
273	75°48.9'	116°46.4'	1603	982.5004	+85.7				219	+1384
277	75°44.9'	116°48.9'	1280	982.5542	+42.7				449	+ 831
279	75°43.2'	116°44.1'	1240	982.5352	+12.7				766	+ 474
282	75°40.6'	116°38.0'	1160	982.5246	-20.7				1095	+ 65
285	75°37.9'	116°32.5'	1110	982.5126	-46.5				1339	- 229
*288/493	75°35.3'	116°27.0'	1116	982 4974	-57.7	- 78.1	0.757	4	1420 b	- 304 b
291/490	75°32.5'	116°22.1'	1069	982.5096	-56.1				1391	- 322
294/487	75°29.5'	116°21.0'	1057	982.4878	-81.4				1801	- 744
297/484	75°26.6'	116°20.0'	1103	982.5206	-32.0				1147	- 44
300/481	75°23.5'	116°17.9'	1141	982.5226	-16.1				989	+ 152
303/478	75°20.4'	116°16.9'	1128	982.5395	- 1.0				792	+ 336
306/475	75°17.4'	116°15.8'	1134	982.5540	+17.6				560	+ 574
309/472	75°14.4'	116°14.5'	1138	982.5543	+21.3				551	+ 587
312/469	75°11.3'	116°13.0'	1085	982.5304	-16.5				1117	- 32
315/466	75°08.3'	116°11.5'	1028	982.5806	+18.2				572	+ 456
318/463	75°05.3'	116°09.7'	971	982.5732	- 4.4				895	+ 76
321/460	75°02.2'	116°08.5'	894	982.5822	-16.8				1046	- 152
*324/457	74°59.4'	116°07.0'	841	982.5754	-38.0	- 33.1	0.723	4	1355 b	- 514 b
327/454	74°56.6'	116°06.0'	819	982.5697	-48.4				1482	- 663
330/451	74°53.6'	116°07.0'	764	982.5822	-50.4				1450	- 686
333/448	74°50.8'	116°09.0'	713	982.6012	-45.3				1316	- 603
336/445	74°48.0'	116°10.0'	651	982.6172	-46.2				1261	- 610
337/444	74°47.0'	116°11.8'	613	982.6329	-38.7				1107	- 494
338/443	74°46 1'	116°12.4'	575	982.6462	-38.8				1069	- 494
339/442	74°45.0'	116°11.2'	546	982.6593	-34.2				969	- 423
340/441	74°43.5'	116°13.3'	509	982.6666	-38.7				997	- 488
342/439	74°42.2'	116°12.5'	472	982.6788	-35.3				905	- 433
345/436	74°39.3'	116°14.0'	362	982.7100	-35.9				796	- 434
348/433	74°36.4'	116°14.5'	258	982.7313	-44.4				803	- 555
351/430	74°33.4'	116°14.7'	141	982.7438	-66.1				1016	- 875
352/429	74°32.4'	116°15.0'	118	982.7527	-63.8				1065	- 847
353/428	74°31.6'	116°15.8'	95	982.7685	-53.0				768	- 673
354/427	74°30.4'	116°16.0'	72	982.7800	-48.5				612 c	- 604
355/426	74°29.6'	116°17.1'	73	982.7703	-56.5				624 c	- 721
356/425	74°28.7'	116°17.5'	75	982.7607	-64.2				648 c	834
357/424	74°27.7'	116°18.0'	76	982.7438	-81.3				660 c	1089
*360/421	74°24.9'	116°18.5'	74	982.7366	-87.0	- 3.9	0.347 (ice bottom) 1.187 (sea bottom)	3	636 b	1167 b
363/418	74°21.9'	116°18.8'	64	982.7329	-91.3				514 c	-1242
366/415	74°18.9'	116°19.2'	65	982.7334	-88.2				526 c	-1207
369/412	74°15.9'	116°20.1'	63	982.7236	-96.3				502 c	-1339
372/409	74°12.9'	116°20.9'	68	982.7352	-80.8				563 c	-1124
375/406	74°10.0'	116°20.5'	60	982.7304	-85.8				465 c	-1209
378/403	74°07.0'	116°20.0'	57	982.7337	-81.0				428 c	-1152
381/400	74°04.1'	116°20.5'	55	982.7472	-65.8				404 c	- 942
384/397	74°01.5'	116°17.5'	44	982.7470	-67.3				269 c	- 976
387/394	73°58.0'	116°14.9'	39	982.7578	-55.3				208 c	- 813
*390.5	73°55.4'	116°11.0'	40	982.7738	-36.9	+ 5.7	0.655 (sea bottom)	2	220 c	- 559 b
496	75°36.3'	116°38.9'	1110	982.5413	-16.5				870	+ 240
499	75°37.0'	116°50.0'	1182	982.5183	-17.7				1033	+ 149
502	75°38.5'	117°01.5'	1232	982.5147	- 7.0				996	+ 236
505	75°39.6'	117°12.5'	1322	982.6131	+11.2				886	+ 436

TABLE 1*a*. (continued)

Station	South Latitude	West Longitude	Surface Elevation (meters a.s.l.)	Observed Gravity (gals)	Free Air Anomaly (milligals)	Bouguer Anomaly (milligals)	Seismic Reflection Time[a] (seconds)	Shot Depth (meters)	Ice Thickness (meters)	Rock Elevation (meters a s l)
508	75°40.5'	117°23.5'	1387	982.4861	+10.7				1033	+ 354
511	75°41.5'	117°35.5'	1423	982.4781	+13.2				1105	+ 318
514	75°42.7'	117°46.5'	1475	982.4531	+ 3.4				1377	+ 98
517	75°43.7'	117°58.0'	1496	982.4536	+ 9.6				1378	+ 118
520	75°44.5'	118°09.5'	1533	982.4482	+16.1				1391	+ 142
523	75°45.5'	118°21.4'	1553	982.4386	+10.9				1563	- 10
526	75°46.6'	118°33.4'	1578	982.4374	+16 7				1574	+ 4
*529	75°47.2'	118°45.0'	1606	982.4349	+22.4	- 39.3	0.846	4	1590 b	+ 16 b
532	75°48.4'	118°56.0'	1626	982.4336	+26.4				1573	+ 53
535	75°49.6'	119°07.5'	1638	982.4261	+21.7				1680	- 42
538	75°50.7'	119°18.5'	1655	982.4126	+12.6				1854	- 199
541	75°52.2'	119°29.5'	1658	982.4111	+11.1				1902	- 244
544	75°53.5'	119°40.5'	1684	982.4153	+22 7				1777	- 93
547	75°54.2'	119°53.0'	1707	982.4302	+43.9				1505	+ 202
550	75°55.3'	120°04.5'	1712	982.3987	+13.0				1746	- 34
553	75°56.1'	120°17.0'	1714	982.4013	+15.7				1980	- 266
556	75°57.0'	120°29.0'	1766	982.3846	+14.4				2074	- 308
559	75°57.6'	120°41.0'	1769	982.3778	+12.1				2134	- 365
562	75°58.5'	120°53.5'	1808	982.3496	- 8.7				2508	- 700
*565	75°59.2'	121°05.0'	1825	982.3320	-21.5	- 25.1	1.448	4	2740 b	- 915 b
568	75°59.0'	121°16.0'	1826	982.3246	-28.5				2795	- 969
571	75°59.2'	121°28.5'	1825	982.3251	-28.4				2742	- 917
574	75°59.4'	121°40.5'	1836	982.3228	-27.4				2687	- 851
577	75°59.6'	121°53.0'	1862	982.3220	-20.4				2558	- 696
580	76°00.0'	122°04.0'	1869	982.3256	-14.9				2432	- 563
583	76°00.4'	122°17.0'	1880	982.3300	- 7.4				2279	- 399
586	76°00.7'	122°28.5'	1918	982.3402	+14.4				1940	- 22
589	76°00.9'	122°40.9'	1930	982.3341	+11.7				1941	- 11
592	76°00.9'	122°53.4'	1921	982.3582	+33.0				1967	- 46
595	76°01.0'	123°05.0'	1970	982.3650	+54.9				1232	+ 738
598	76°01.0'	123°17.5'	2031	982.3419	+50.7				1306	+ 725
601	76°00.7'	123°30.0'	2034	982.3401	+49.9				1270	+ 764
*603	76°01.0'	123°42.0'	2074	982.3550	+77.0		N R.		852	+1222
606	76°01.0'	123°53.5'	2075	982.3412	+63.5				1005	+1070
609	76°01.9'	124°05.7'	2072	982.3745	+94.2				491	+1581
*612.3	76°00.8'	124°18.5'	2074	982.3517	+73.8	-103.4	0.414	3	763 b	+1311 b
615	76°00.0'	124°28.7'	2026	982.3440	+52.0				1069	+ 957
618	75°57.9'	124°37.9'	1981	982.3181	+13.5				1629	+ 352
621	75°55.6'	124°46.0'	1958	982.3035	- 6.5				1932	+ 26
624	75°53.4'	124°54.6'	1937	982.3247	+ 9.9				1693	+ 244
627	75°51.4'	125°03.8'	1818	982.3530	+ 2.8				1707	+ 111
630	75°49.1'	125°12.2'	1804	982.3405	-12.3				1946	- 142
633	75°47.0'	125°20.5'	1763	982.3804	+16.5				1501	+ 262
636	75°44.7'	125°29.8'	1653	982.3983	+ 2.1				1733	- 80
*639	75°42.7'	125°38.1'	1647	982.3780	-18.5	- 58.6	1.038	3	1955 b	- 308 b
642	75°43.2'	125°50.2'	1673	982.3719	-17.0				1926	- 253
645	75°44.0'	126°01.5'	1732	982.3588	-12.6				1887	- 155
648	75°44.5'	126°13.6'	1795	982.3567	+ 4.3				1665	+ 130
651	75°45.4'	126°25.0'	1826	982.3648	+22.1				1397	+ 429
654	75°45:6'	126°37.7'	1899	982.3510	+30.7				1309	+ 590
657	75°46.3'	126°49.5'	1908	982.3582	+39.5				1153	+ 755
660	75°47.0'	127°01.2'	1986	982.3352	+40.1				1190	+ 796
663	75°48.0'	127°12.5'	2023	982.3488	+64.4				831	+1192
666	75°49.0'	127°24.0'	1988	982.3605	+64.5				762	+1226
669	75°48.5'	'27°36.0'	1954	982.3503	+44.2				1000	+ 954
672	75°48.0'	_27°48.0'	1954	982.3555	+50.8				869	+1085
*676	75°47.5'	128°04.0'	1964	982.3615	+59.2	-111.2	0.407	5	710 b	+1254 b
678	75°47.8'	128°12.0'	2003	982.3674	+76.9				489	+1514
681	75°48.0'	128°24.3'	1892	982.4011	+80.8				326	+1566
684	75°48.3'	128°37.0'	1928	982.4036	+89.7				234	+1694
687	75°48.8'	128°43.0'	2021	982.3948	+106.5				87	+1934
690	75°50.6'	128°53.5'	1932	982.3678	+52.4				815	+1117
693	75°52.4'	129°03.5'	1894	982.3490	+19.6				1275	+ 619
696	75°53.1'	129°16.0'	1891	982.3271	- 1.6				1596	+ 295
699	75°55.0'	129°26.0'	1888	982.3331	+ 1.9				1546	+ 342
702	75°56.9'	129°37.0'	1846	982.3344	-11.1				1705	+ 141
705	75°58.6'	129°47.0'	1842	982.3348	-13.1				1737	+ 105
708	75°59.9'	130°00.0'	1838	982.3497	- 0.4				1542	+ 296
*711.5	76°02.0'	130°08.0'	1874	982.3541	+13.8	- 94.9	0.734	3	1370 b	+ 504 b
714	76°02.6'	130°18.9'	1879	982.3464	+ 7.2				1488	+ 391
717	76°05.0'	130°29.7'	1893	982.3530	+16.4				1378	+ 515
720	76°06.7'	130°40.0'	1896	982.3529	+16.0				1401	+ 495
723	76°08.4'	130°51.0'	1903	982.3254	- 9.9				1810	+ 93

TABLE 1*a*. (continued)

Station	South Latitude	West Longitude	Surface Elevation (meters a.s.l.)	Observed Gravity (gals)	Free Air Anomaly (milligals)	Bouguer Anomaly (milligals)	Seismic Reflection Time[a] (seconds)	Shot Depth (meters)	Ice Thickness (meters)	Rock Elevation (meters a.s.l.)
726	76°09.8'	131°01.9'	1908	982.3066	-28.2				2104	- 196
729	76°11.4'	131°12.5'	1942	982.3001	-26.1				2120	- 178
732	76°12.6'	131°24.0'	1948	982.2823	-42.7				2389	- 441
735	76°14.3'	131°34.5'	1963	982.2937	-28.0				2198	- 235
738	76°15.7'	131°45.0'	2003	982.3026	- 7.7				1947	+ 56
741	76°17.3'	131°56.0'	2048	982.2991	+ 1.5				2030	+ 18
744	76°18.8'	132°07.0'	2121	982.2882	+22.1				1646	+ 475
*747	76°20.3'	132°18.0'	2143	982.2980	+27.8	- 94.5	0.849	3	1594 b	+ 549 b
750	76°22.0'	132°28.0'	2140	982.2962	+46.2				1326	+ 814
753	76°23.6'	132°38.5'	2139	982.2981	+24.4				1663	+ 476
756	76°25.0'	132°50.0'	2159	982.3136	+45.0				1385	+ 774
759	76°26.5'	133°01.0'	2167	982.3141	+47.0				1374	+ 793
762	76°28.2'	133°12.0'	2169	982.2986	+31.0				1627	+ 542
765	76°29.7'	133°23.0'	2175	982.2956	+28.8				1666	+ 509
768	76°31.0'	133°34.0'	2174	982.2893	+21.3				1800	+ 374
771	76°32.5'	133°45.0'	2183	982.3009	+34.7				1619	+ 564
774	76°34.0'	133°56.5'	2194	982.2864	+22.5				1824	+ 370
777	76°35.5'	134°07.6'	2187	982.3025	+35.4				1634	+ 553
780	76°36.9'	134°18.7'	2177	982.3053	+34.1				1655	+ 522
*783	76°38.3'	134°30.0'	2160	982.3074	+30.1	- 85.4	0.909	3	1709 b	+ 451 b
786	76°39.6'	134°41.4'	2174	982.3003	+18.1				1882	+ 292
789	76°40.9'	134°53.5'	2129	982.3091	+20.4				1781	+ 348
792	76°42.2'	135°05.0'	2117	982.3099	+16.7				1803	+ 314
795	76°43.6'	135°16.9'	2077	982.3325	+26.0				1603	+ 474
798	76°45.0'	135°28.2'	2061	982.3465	+34.1				1444	+ 617
801	76°46.3'	135°40.0'	2033	982.3517	+29.8				1459	+ 574
804	76°47.5'	135°52.0'	2019	982.3371	+10.1				1720	+ 299
807	76°48.8'	136°04.0'	1994	982.3705	+34.8				1303	+ 691
810	76°50.3'	136°16.0'	1974	982.3754	+32.6				1295	+ 679
813	76°51.6'	136°27.5'	1926	982.3978	+39.3				1125	+ 801
816	76°52.8'	136°40.0'	1895	982.4022	+33.3				1163	+ 732
*819	76°54.0'	136°52.0'	1849	982.3967	+12.8	- 90.6	0.749	3	1403 b	+ 446 b
822	76°55.2'	137°04.0'	1846	982.3870	+ 1.9				1568	+ 278
825	76°56.4'	137°16.5'	1809	982.4333	+35.5				1032	+ 777
828	76°57.7'	137°28.5'	1775	982.4450	+36.3				991	+ 784
831	76°59.2'	137°40.0'	1749	982.4241	+ 5.9				1425	+ 324
834	77°05.0'	137°51.8'	1741	982.4304	+ 5.9				1422	+ 319
837	77°01.7'	138°04.0'	1717	982.4487	+19.0				1206	+ 511
840	77°02.9'	138°16.5'	1686	982.4819	+41.8				838	+ 848
843	77°04.1'	138°29.0'	1642	982.4949	+40.5				818	+ 824
846	77°05.2'	138°41.2'	1626	982.4796	+19.5				1122	+ 504
849	77°06.3'	138°53.5'	1628	982.4951	+34.9				898	+ 730
852	77°07.6'	139°06.0'	1572	982.5230	+44.7				699	+ 873
*855	77°09.0'	139°18.0'	1514	982.5165	+19.3	- 74.5	0.550	5	1027 b	+ 487 b
858	77°10.0'	139°30.5'	1509	982.4731	-26.2				1675	- 166
861	77°11.4'	139°43.0'	1511	982.4837	-16.0				1517	- 6
864	77°12.4'	139°55.5'	1489	982.5107	+ 3.7				1149	+ 340
867	77°13.4'	140°08.4'	1464	982.4710	-44.5				1818	- 354
870	77°14.5'	140°21.0'	1449	982.5388	+18.1				835	+ 614
873	77°15.5'	140°33.5'	1427	982.5637	+35.5				523	+ 904
876	77°16.6'	140°46.0'	1384	982.5624	+20.2				680	+ 704
879	77°17.6'	140°59.0'	1323	982.5960	+34.4				377	+ 946
882	77°18.7'	141°11.5'	1248	982.6015	+16.0				550	+ 698
885	77°19.7'	141°24.8'	1166	982.6078	- 3.7				734	+ 432
888	77°20.8'	141°37.5'	1113	982.6254	- 3.2				644	+ 469
*890	77°21.5'	141°46.0'	1107	982.6227	- 8.2	- 81.2	0.376	5	694 b	+ 413 b
894	77°24.8'	141°35.0'	1118	982.5825	-47.2				1350	- 232
897	77°27.1'	141°26.5'	1161	982.5778	-39.9				1328	- 167
900	77°29.4'	141°17.7'	1197	982.5647	-43.5				1328	- 131
903	77°31.5'	141°08.0'	1200	982.5512	-57.4				1720	- 520
906	77°33.7'	140°59.5'	1205	982.5497	-58.6				1788	- 583
909	77°36.3'	140°51.0'	1204	982.5736	-36.8				1505	- 301
912	77°38.5'	140°42.0'	1210	982.5951	-14.9				1228	- 18
915	77°41.0'	140°32.5'	1192	982.5883	-28.7				1462	- 270
918	77°43.3'	140°24.0'	1166	982.5861	-40.5				1658	- 492
921	77°45.6'	140°15.7'	1148	982.5769	-56.7				1928	- 780
924	77°48.0'	140°06.5'	1140	982.5585	-79.0				2299	-1159
*927	77°50.3'	139°57.0'	1140	982.5409	-98.1	- 34.9	1.370	5	2630 b	-1490 b
930	77°52.5'	139°47.5'	1145	982.4994	-139.4				3166	-2021
933	77°55.0'	139°38.5'	1130	982.5201	-124.9				2846	-1716
936	77°57.3'	139°30.0'	1150	982.5115	-128.7				2834	-1684
939	77°59.7'	139°21.0'	1151	982.5290	-112.4				2503	-1352
942	78°02.0'	139°12.0'	1143	982.5724	-72.9				1814	- 671

TABLE 1*a*. (concluded)

Station	South Latitude	West Longitude	Surface Elevation (meters a.s.l.)	Observed Gravity (gals)	Free Air Anomaly (milligals)	Bouguer Anomaly (milligals)	Seismic Reflection Time[a] (seconds)	Ice Thickness (meters)	Shot Depth (meters)	Rock Elevation (meters a.s.l.)
945	78°04.1'	139°02.2'	1131	982.6065	-43.7			1276		- 145
948	78°06.5'	138°53.5'	1112	982.6132	-44.3			1178		- 66
951	78°09.0'	138°45.0'	1064	982.6084	-65.2			1355		- 291
954	78°11.4'	138°36.0'	1059	982.5678	-109.2			1922		- 863
957	78°13 8'	138°27.5'	1050	982.5501	-131.1			2153		-1103
960	78°16 3'	138°18.6'	1062	982.5463	-132.7			2101		-1039
*963	78°18 7'	138°10.0'	1065	982.5953	-84.1	-108.4	0.687	1288 b	5	- 223 b
966	78°21.1'	138°01.8'	1063	982.6348	-46.7			847		+ 216
969	78°23 6'	137°53.0'	1020	982.6594	-36.8			778		+ 242
972	78°26.0'	137°44.5'	1036	982.6416	-51.2			1132		- 96
975	78°28 5'	137°34.0'	1037	982.6669	-27.0			891		+ 146
978	78°30.7'	137°24.4'	1039	982.6802	-14.4			827		+ 212
981	78°33.0'	137°15.0'	1013	982.6888	-15.2			935		+ 78
984	78°35.5'	137°05.5'	994	982.6943	-17.1			1066		- 72
987	78°37.8'	136°57.0'	987	982.6893	-25.5			1307		- 320
990	78°40.3'	136°46.5'	961	982.6951	-29.2			1459		- 498
993	78°42.5'	136°36.5'	915	982.6837	-56.1			1938		-1023
996	78°45.0'	136°26.5'	940	982.7003	-33.2			1742		- 802
#*998/AN400	78°45.4'	136°17.0'	946	982.7011	-30.9	- 0.6		1835 b		- 889 b
1002/AN405	78°45.0'	135°55.0'	990	982.7040	-14.7			1596		- 606
1007/AN410	78°44.6'	135°32.5'	1039	982.6787	-23.0			1690		- 651
1011/AN415	78°44.2'	135°10.0'	1041	982.6683	-34.0			1858		- 817
1015/AN420	78°43.8'	134°48.0'	1066	982.6806	-12.8			1525		- 459
*1020/AN425	78°43.4'	134°25.5'	1126	982.6694	- 5.3	- 25.1	0.763	1432 b	4	- 306 b
1024/AN430	78°42.9'	134°03.5'	1165	982.6403	-22.5			1760		- 595
1028/AN435	78°42.3'	133°41.0'	1159	982.6451	-18.7			1728		- 569
1033/AN440	78°41.7'	133°19.5'	1186	982.6422	-13.6			1710		- 524
1037/AN445	78°41.1'	132°57.0'	1216	982.6083	-37.9			2136		- 920
# 1041/AN450	78°41.5'	132°34.2'	1253	982.5934	-40.6	- 14.2		2245 b		- 992 b
1046/AN455	78°39.8'	132°13.5'	1267	982.5920	-37.7			2174		- 907
1050/AN460	78°39.0'	131°53.0'	1293	982.5910	-30.7			2054		- 761
1054/AN465	78°38 3'	131°31.7'	1314	982.5744	-39.3			2162		- 848
1059/AN470	78°37.4'	131°10.5'	1347	982.5563	-47.4			2275		- 928
* 1063/AN475	78°36.5'	130°49.5'	1388	982.5536	-36.9	- 35.1	1.121	2117 b	5	- 729 b
1067/AN480	78°35.6'	130°28.0'	1403	982.5720	-13.1			1802		- 399
1072/AN485	78°38.7'	130°09.0'	1415	982.5939	+10.8			1411		+ 4
1076/AN490	78°41.6'	129°51.0'	1407	982.5830	- 4.3			1729		- 322
1080/AN495	78°44.4'	129°32.0'	1403	982.5998	+ 8.1			1566		- 163
# 1085/AN500	78°47.4'	129°13.0'	1428	982.5872	+ 2.3	- 30.9		1705 b		- 277 b
1089/AN505	78°50.0'	128°56.5'	1436	982.5713	-11.5			1964		- 528
1093/AN510	78°52.5'	128°39.5'	1441	982.5643	-19.2			2129		- 688
1098/AN515	78°55.2'	128°22.5'	1480	982.5792	+ 6.5			1889		- 409
# 1102/AN520	78°57.8'	128°06.0'	1494	982.5992	+29.7	- 23.6		1535 b		- 41 b
1106/AN525	79°00.4'	127°49.0'	1505	982.6038	+35.7			1496		+ 9
1111/AN530	79°04.6'	127°32.0'	1501	982.6126	+41.1			1452		+ 49
1115/AN535	79°05.3'	127°14.4'	1486	982.6083	+30.1			1643		- 157
# 1119/AN540	79°07.8'	126°57.0'	1481	982.5899	+10.2	- 8.9		1975 b		- 494 b
1124/AN545	79°10.5'	126°38.0'	1479	982.5856	+ 4.3			2066		- 587
1128/AN550	79°13.2'	126°19.0'	1476	982.5845	+ 0.5			2127		- 651
1132/AN555	79°15.9'	126°01.0'	1467	982.5851	- 3.1			2177		- 710
# 1137/AN560	79°18.4'	125°42.0'	1464	982.5840	- 5.8	- 4.9		2220 b		- 756 b
1141/AN565	79°21.1'	125°23.0'	1451	982.5883	- 7.2			2231		- 780
1145/AN570	79°23.7'	125°03.0'	1447	982.5926	- 6.5			2219		- 772
1150/AN575	79°26.2'	124°44.0'	1449	982.5910	- 7.8			2245		- 796
# 1154/AN580	79°28.6'	124°24.0'	1453	982.5923	- 6.3	- 3.4		2230 b		- 777 b
1158/AN585	79°31.1'	124°04.5'	1439	982.5936	-11.6			2365		- 926
1163/AN590	79°33.4'	123°45.5'	1435	982.5974	-10.4			2413		- 978
1167/AN595	79°35.7'	123°26.4'	1449	982.5971	- 5.4			2423		- 974
# 1171/AN600	79°38.1'	123°06.4'	1443	982.6022	- 4.0	+ 17.4		2465 b		-1022 b
1176/AN605	79°40.4'	122°46.0'	1458	982.5979	- 6.4			2460		-1002
1180/AN610	79°42.7'	122°26.0'	1476	982.5942	- 5.5			2408		- 932
1184/AN615	79°45.0'	122°06.0'	1473	982.5950	- 6.4			2363		- 890
#1189/AN620	79°47.2'	121°46.0'	1478	982.5920	-10.5	+ 0.4		2375 b		- 897 b
1193/AN625	79°49.7'	121°25.0'	1492	982.5819	-17.5			2574		-1082
1197/AN630	79°52.1'	121°04.0'	1503	982.5790	-18.8			2685		-1182
1202/AN635	79°53.5'	120°51.8'	1510	982.5886	- 3.4			2540		-1030
1206/AN640	79°57.0'	120°22.0'	1523	982.5910	- 3.0			2627		-1104
1211/AN646 (Byrd)	79°59.2'	120°01.0'	1525	982.5960	+ 2.4	+ 28.0		2645 b		-1120 b

*Seismic station

#Seismic station, Little America-Byrd traverse, 1957

[a]Corrected to bottom of shot hole

[b]Determined from seismic reflection

[c]Determined from surface elevation

TABLE 1*b*. Station Positions and Elevations, Executive Committee Range Traverse, Excluding Segment Common with Marie Byrd Land Traverse

Station	South Latitude	West Longitude	Elevation (meters a.s.l.)	Station	South Latitude	West Longitude	Elevation (meters a.s.l.)
164	77°13.0'	119°51'	1883	313	77°49.6'	124°32'	1769
167	77°12.7'	120°04'	1910	316	77°52.4'	124°27'	1772
170	77°12.4'	120°18'	1916	319	77°55.1'	124°21'	1771
173	77°12.1'	120°31'	1936	322	77°57.8'	124°15'	1769
176	77°11.8'	120°44'	1951	325	78°00.5'	124°10'	1754
179	77°11.5'	120°58'	1960	328	78°03.2'	124°04'	1719
182	77°11.2'	121°11'	1966	331	78°06.0'	123°58'	1702
185	77°11.0'	121°25'	1979	334	78°08.7'	123°52'	1687
188	77°10.7'	121°38'	1990	337	78°11.4'	123°47'	1674
191	77°10.4'	121°51'	2007	340	78°14.1'	123°41'	1666
194	77°10.1'	122°05'	2020	343	78°16.8'	123°35'	1666
197	77°09.8'	122°18'	2017	346	78°19.5'	123°30'	1646
200	77°09.5'	122°31'	2025	349	78°22.2'	123°24'	1639
203	77°09.2'	122°45'	2037	352	78°25.0'	123°18'	1621
206	77°08.9'	122°58'	2042	355	78°27.7'	123°13'	1619
209	77°08.6'	123°11'	2057	358	78°30.4'	123°07'	1594
212	77°08.3'	123°25'	2054	361	78°33.1'	123°01'	1585
215	77°08.0'	123°38'	2048	364	78°35.9'	122°56'	1584
218	77°07.7'	123°51'	2050	367	78°38.6'	122°50'	1568
221	77°07.5'	124°05'	2045	370	78°41.3'	122°44'	1582
224	77°07.2'	124°18'	2079	373	78°44.0'	122°38'	1569
227	77°06.9'	124°32'	2083	376	78°46.7'	122°33'	1565
230	77°06.6'	124°45'	2098	379	78°49.4'	122°27'	1567
233	77°06.3'	124°58'	2080	382	78°52.2'	122°21'	1555
236	77°06.0'	125°12'	2107	385	78°54.9'	122°16'	1548
239	77°05.7'	124°25'	2076	388	78°57.6'	122°10'	1538
242	77°02.9'	124°31'	2175	391	79°00.3'	122°04'	1532
245	77°00.2'	124°36'	2126	394	79°03.0'	121°59'	1530
248	76°57.4'	125°42'	2256	397	79°05.7'	121°53'	1526
251	76°54.6'	125°48'	2297	400	79°08.5'	121°47'	1524
254	76°57.4'	125°42'	2256	403	79°11.2'	121°42'	1527
257	77°00.2'	125°36'	2126	406	79°13.9'	121°36'	1519
260	77°02.9'	125°31'	2175	409	79°16.6'	121°30'	1516
263	77°05.7'	125°25'	2076	412	79°19.3'	121°24'	1512
266	77°07.7'	125°34'	2035	415	79°22.1'	121°19'	1500
269	77°09.6'	125°43'	1973	418	79°24.8'	121°13'	1493
271	77°11.6'	125°52'	1943	421	79°27.5'	121°07'	1491
274	77°14.3'	125°46'	1938	424	79°30.2'	121°02'	1486
277	77°17.0'	125°41'	1927	427	79°32.9'	120°56'	1490
280	77°19.8'	125°35'	1931	430	79°35.6'	120°50'	1500
283	77°22.5'	125°29'	1920	433	79°38.4'	120°45'	1500
286	77°25.2'	125°23'	1916	436	79°41.1'	120°39'	1500
289	77°27.9'	125°18'	1891	439	79°43.8'	120°33'	1490
292	77°30.6'	125°12'	1877	442	79°46.5'	120°28'	1503
295	77°33.3'	125°06'	1824	445	79°49.2'	120°22'	1514
298	77°36.1'	125°01'	1822	448	79°52.0'	120°16'	1509
301	77°38.8'	124°55'	1809	451	79°54.7'	120°10'	1525
304	77°41.5'	124°49'	1815	454	79°57.4'	120°05'	1521
307	77°44.2'	124°44'	1790	Byrd	79°59.2'	120°01'	1525
310	77°46.9'	124°38'	1800				

TABLE 1c. Station Positions, Elevations, and Seismic Results, Last Part of Horlick Mountains Traverse

Station	South Latitude	West Longitude	Surface Elevation (meters a.s.l.)	Seismic Reflection Time (seconds)	Ice Thickness (meters)	Rock Elevation (meters a.s.l.)
747	82°08.6'	109°14'	1808	1.185	2230	- 422
750	82°06.6'	109°28'	1783			
753	82°04.6'	109°43'	1787			
756	82°02.6'	109°57'	1774			
759	82°00.6'	110°11'	1753			
762	81°58.6'	110°26'	1738			
765	81°56.6'	110°40'	1747			
768	81°54.5'	110°54'	1752			
771	81°52.5'	111°09'	1738			
774	81°50.5'	111°23'	1717			
777	81°48.5'	111°37'	1703			
780	81°46.5'	111°52'	1690			
783	81°44.5'	112°06'	1684	1.274	2405	- 721
787	81°41.6'	112°22'	1678			
791	81°38.7'	112°39'	1655			
795	81°35.8'	112°56'	1640			
799	81°32.9'	113°12'	1612			
803	81°29.9'	113°28'	1595			
807	81°27.0'	113°45'	1600			
811	81°24.1'	114°02'	1600			
815	81°21.2'	114°18'	1608	1.390	2625	-1017
819	81°18.1'	114°34'	1574			
823	81°15.0'	114°51'	1554			
827	81°11.9'	115°08'	1522			
831	81°08.8'	115°24'	1512			
833	81°07.2'	115°32'	1521			
835	81°05.6'	115°40'	1517			
835.5	81°06.0'	115°42'	1516			
839	81°02.5'	115°57'	1510			
843	80°59.4'	116°14'	1492			
847	80°56.3'	116°30'	1490	1.490	2815	-1335
851	80°53.3'	116°41'	1489			
855	80°50.3'	116°53'	1503			
859	80°47.2'	117°04'	1497			
863	80°44.2'	117°16'	1513			
867	80°41.2'	117°27'	1505			
871	80°38.2'	117°38'	1526			
875	80°35.2'	117°50'	1530			
879	80°32.1'	118°01'	1519			
883	80°29.1'	118°13'	1524	1.266	2390	- 885
887	80°26.1'	118°24'	1505			
891	80°22.7'	118°36'	1486			
895	80°19.4'	118°48'	1483			
899	80°16.0'	118°01'	1478			
903	80°12.7'	118°13'	1492			
907	80°09.3'	118°25'	1494			
911	80°05.9'	118°38'	1501			
915	80°02.6'	118°50'	1523			
Byrd	79°59.2'	120°02'	1525		2645	-1120

Gravity

Considerable difficulty was encountered in reducing the gravity data. The first problem was the correction for the gravimeter temperature variations, which covered the range 68–72°F (20–22°C). To determine the effect of temperature on instrument reading, Parks conducted controlled experiments during the winter of 1960 at Byrd station. Gravimeter dial readings and thermometer indications from field stations where there was more than one reading were also compared. The latter data were in good agreement with the coefficient of 5.3 mgal/°F (9.5 mgal/°C) indicated by the observations at Byrd station (Figure 4). Field measure-

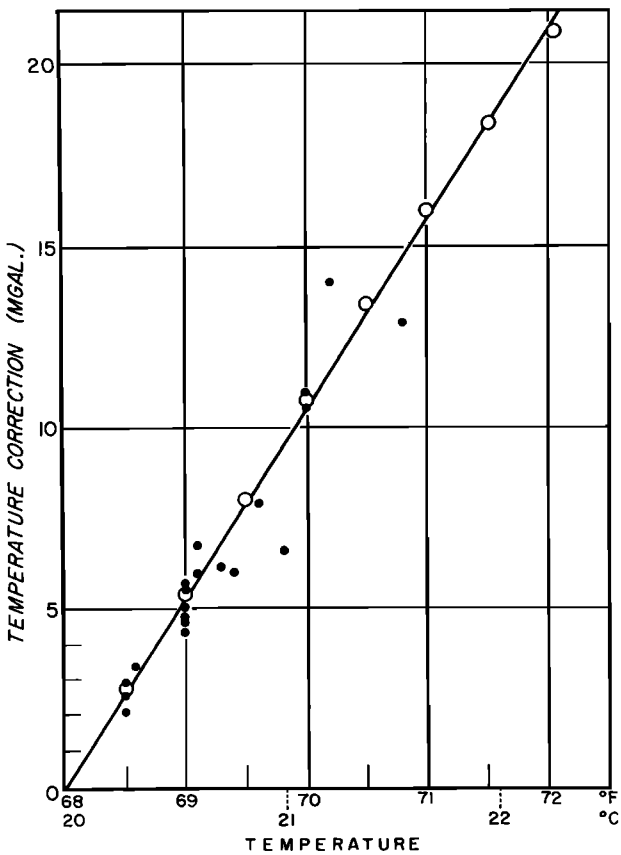

Fig. 4. Temperature calibration of gravimeter. Dots indicate field observations; open circles indicate observations at Byrd station.

ments were complicated by a lag between temperature changes at the thermometer and the corresponding internal changes affecting instrument readings. This is illustrated in Figure 5, which shows a typical variation of indicated gravity reading with time, the indicated temperature being written at points along the curve. The error in observed gravity resulting from temperature instability (and from a thermometer reading error of about ±0.1°F) was estimated from Figure 5 to be less than ±5 mgal.

Another problem resulted from irregular drift. Two tares, probably caused by temperature shocks to the instrument, occurred while at a station and could thus be corrected for: a decrease of 9 mgal at station 258, and an increase of 5 mgal at station 855. Between stations 186 and 189, an unreasonably large apparent change of 60 mgal was attributed to a tare, since it occurred in a region of otherwise moderate gravity gradients. By computing gravity differences from the end of the traverse to station 189, and from the beginning to station 186, a much more modest change of 3.4 mgal was obtained. This correction greatly improved the agreement between the values for the difference in ice thickness between station 168 and station 198 as computed from seismic soundings and free-air anomalies, respectively.

An airlifted tie from Byrd station to station 783 was made with a Worden gravimeter by E. C. Thiel on January 21. From this point to the junction of the traverse with the Army-Navy Drive, there was a misclosure of 9.2 mgal. Correction for this was applied linearly along this section of the traverse. Gravity values were adjusted to fit previously measured values (*Bentley and Ostenso* [1961], adjusted for the most recent value of 982.5960 given for Byrd station by *Woollard and Rose* [1963]) at the junction with Army-Navy Drive (station AN400) and at Byrd station, but not elsewhere along this trail. Because of the instrumental difficulties encountered on the Marie Byrd Land traverse, the adjusted gravity values from the Little America–Byrd traverse are believed to be more reliable, and are listed in Table 1 with a few minor corrections.

Free-air gravity anomalies were calculated for all

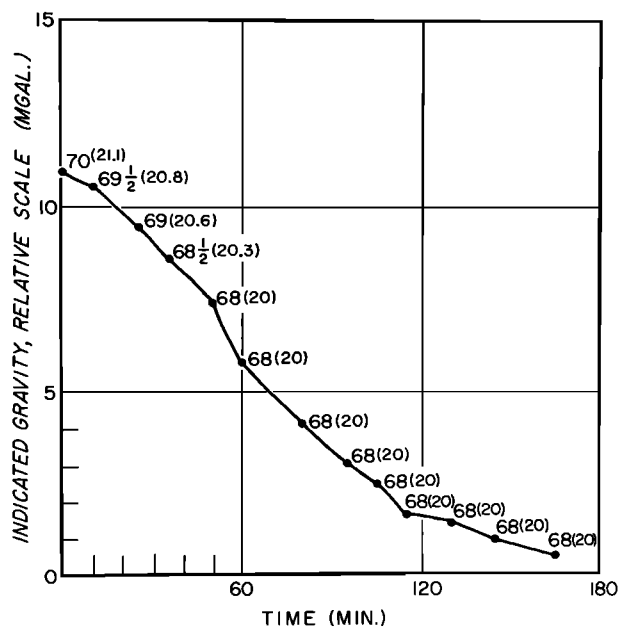

Fig. 5. Typical variation of indicated gravity reading with the time and temperature. Temperature in °F is noted next to each observed point.

stations. At those stations where the ice thickness was measured, 'ice-corrected' Bouguer anomalies were computed, i.e. correction was made for the entire ice column, using a density of 0.9 g/cm^3, and then for the remaining surplus or deficit of rock mass relative to sea level, assuming a density of 2.67 g/cm^3. This is the same as a simple Bouguer correction applied for the equivalent elevation of the rock, i.e. the elevation of a land surface that would have the same load above a given level as that of the actual rock and superimposed ice combined.

It is clear from the previous discussion that the observed gravity values could be in error by 10 mgal or more along some sections of the traverse. The error in gravity anomalies could reach 20 mgal, although the relative error between adjacent stations would be substantially less.

Ice Thickness

The ice thickness at each seismic station (Table 1) was computed assuming an average velocity of 3820 m/sec for vertically traveling waves beneath the near-surface low-velocity firn. A constant negative correction of 30 meters was applied to the computed ice thickness values to allow for the near-surface low velocities. The average velocity beneath these layers was computed by *Bentley and Ostenso* [1961] assuming a velocity of 3850 m/sec through 90% of the ice, and 3600 m/sec in the lowest 10%. A maximum error of ±40 meters in total ice thickness, caused chiefly by uncertainty in the thickness of the basal low velocity layer, was estimated. The velocity of 3840 ± 25 m/sec obtained in the ice near Toney Mountain [*Chang*, 1964] is in good agreement with the earlier measurements.

Free-air gravity anomalies were used to interpolate rock elevation between seismic reflection stations. To determine the best conversion factor to use, a plot of the difference in rock elevation between seismic stations versus the difference in free-air gravity anomaly between the same stations was prepared (Figure 6). Omitting extreme values, a least-squares regression line with slope 16.2 m/mgal was fitted to the majority of the points (solid points in Figure 6), which were considered to be representative of the area as a whole. The slope was rounded off to 15 m/mgal; it is clear from the scatter of the points in Figure 6 that this is not significantly different from the computed value. The points represented by open circles were omitted from the determination of slope as having too great an effect on the least-squares computation compared with their actual importance in the analysis. Since very large elevation differences are almost surely connected with relative maxima and minima in rock height, the associated difference in gravity anomaly would probably be unrealistically small, owing to the effect of the surrounding subglacial terrain. The points indicated by crosses are simply extreme deviations from the norm. The root-mean-square deviation of elevation differences from the 15-m/mgal relation is 230 meters excluding these points and 440 meters including them.

On the assumption that a 1-mgal anomaly represents a 15-meter change in rock level, the change in rock elevation equivalent to the change in free-air anomaly relative to the nearest preceding seismic station was calculated for each gravity station. The difference between the rock elevation computed from the free-air anomaly and that computed from seismic soundings at the next seismic station was distributed linearly among the gravity stations. In regions of rough rock topography, the probable error in this process is clearly several hundred meters.

An empirical relation between surface elevation and thickness of the floating ice shelf was determined from the differences between the elevation and ice thickness (from seismic reflections) at station 360, and the elevation (43 meters) and ice thickness (257 meters) at Little America station [*Crary et al.*, 1962]. The resulting factor—change in ice thickness equals 11 times change in elevation—was used between station 354 and the Amundsen Sea. Ocean bottom depths were determined from seismic reflections at stations 360 and 390.5, assuming a wave velocity in the sea water of 1.44 km/sec. Depths elsewhere were determined from the free-air anomalies assuming a specific gravity of 1.03 for sea water and 2.67 for rock.

Magnetometry

Since the small change in calibration constant of the magnetometer between departure from and return to Byrd station was not significant in view of the over-all uncertainties in the magnetic observations, a mean factor of 27.5 γ/scale division was used for the whole magnetic profile. The profile was computed from the readings with the magnetometer ori-

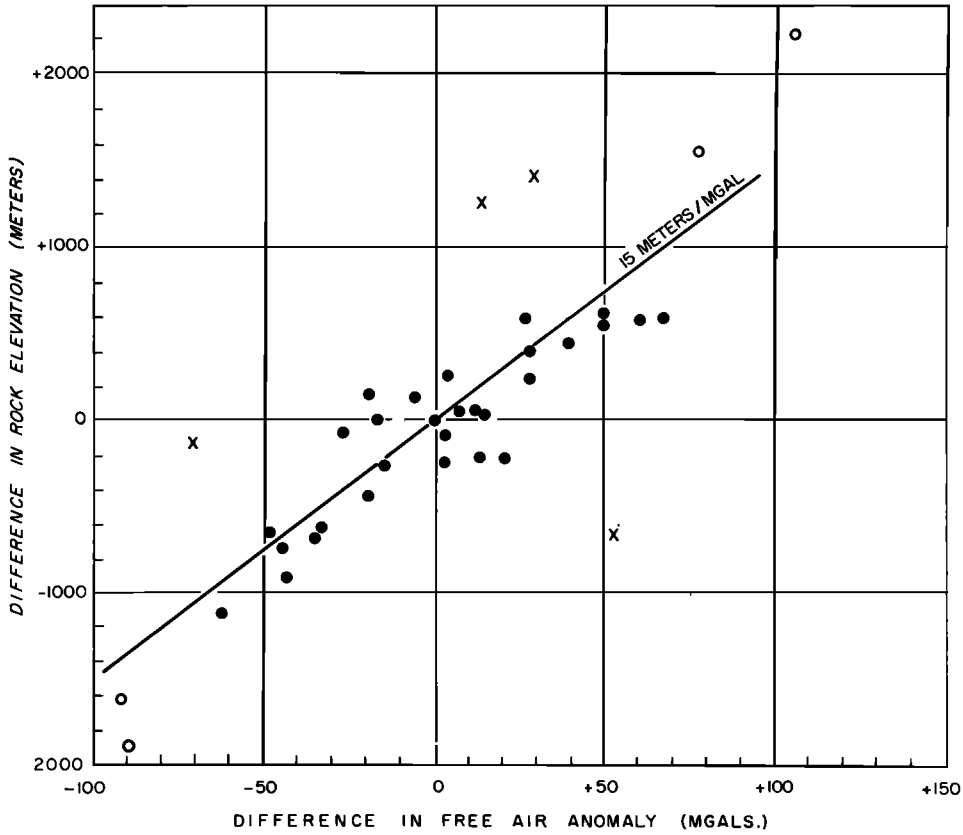

Fig. 6. Comparison of differences in free-air anomalies and rock elevation between seismic stations. Open circles indicate points not used in regression slope determination; crosses indicate points separately considered in error estimation.

ented southward, since this was the orientation for the repeated observations at seismic stations.

An estimate of the accuracy of the magnetic observations was derived from the readings obtained with northward and southward orientation of the magnetometer. The mean difference between readings was 550 γ (attributable to an error of about 1° in the level bubble) with a standard error of ± 75 γ. The corresponding error in an individual reading is thus $75/\sqrt{2} \simeq 50$ γ. (A reduction in the error by another factor of $\sqrt{2}$ could have been gained by computing the profile using the mean of the two readings; in view of other errors, this insignificant improvement was clearly not worth the computational effort.)

No corrections were applied for temporal magnetic variations, previous experience having shown the futility of doing so with control stations hundreds of kilometers away [*Ostenso and Bentley*, 1959]. The raw readings, multiplied by the calibration factor and adjusted to the station value at Byrd station at the time of departure (58,560 γ at 1935 GMT on November 5, 1959 [*U.S. Coast and Geodetic Survey*, 1962]), are shown in Figure 7. A closure error of approximately 1000 γ was immediately apparent. Correction for the jump of 500 γ between stations 526 and 529 (975 km along the traverse) reduced this error by half. It was further found that a regional gradient could much more satisfactorily be fitted to the observed profile if another instrumental jump of 500 γ was assumed to have occurred between stations 87 and 96 (160–180 km along the traverse), the closure error at the same time being eliminated. Although there was no field evidence for such a tare, the assumption was adopted as the most satisfactory explanation of the observations. The resulting regional magnetic curve, shown by the dashed line in Figure 7, was used to construct the regional map of vertical intensity (Figure 8).

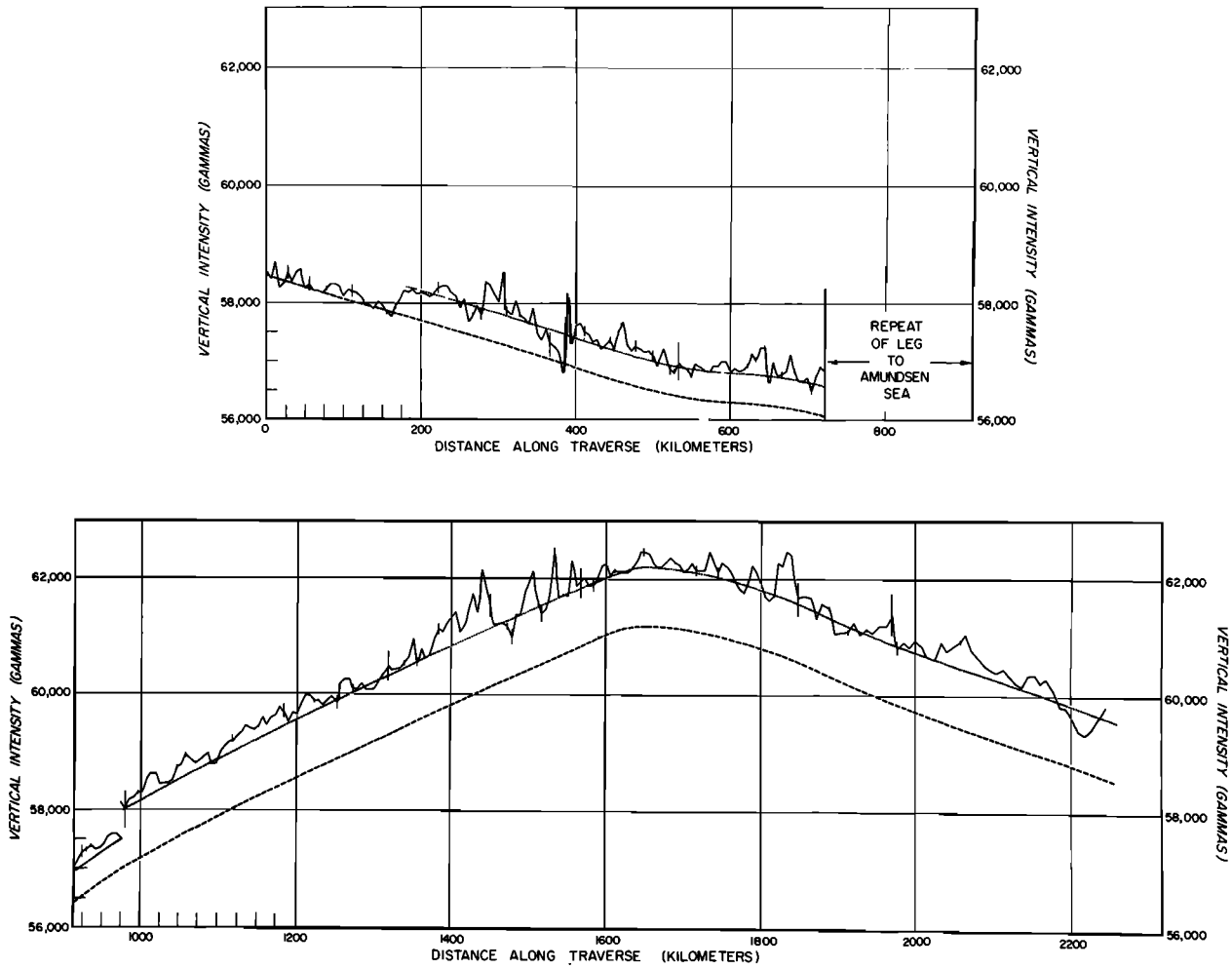

Fig. 7. Observed vertical magnetic intensity. Upper and lower dotted lines indicate regional curves fitted before and after tare corrections, respectively. Vertical line segments show the range of observed values at seismic stations.

The regional field has been removed from the observed vertical intensity values to produce the anomaly profile shown in Figure 9. To provide a guide in interpreting the variations in vertical intensity, we have superimposed on the profile a series of lines indicating the level of activity at Byrd station during the times of measurement. The height of each line segment above the zero line gives the difference, to the nearest 50 γ, between the maximum and minimum value of vertical intensity recorded at Byrd station during the period starting three hours before the initial field observation and ending three hours after the last field observation for each continuous interval of travel. Thus anomalies that substantially exceed the corresponding activity level in amplitude can be regarded with confidence as resulting from geologic sources, whereas those of lesser amplitude may very well result from ionospheric activity alone.

For the repeated section of the traverse from mile 288 to mile 390.5, the Z values from the outgoing leg have been used, since the activity level for the return trip was much higher, 450 to 650 γ. Nevertheless, the agreement between repeated observations was within ± 200 γ at all stations, reproducing in gross the 500 γ anomaly observed along this section of the route.

RESULTS

The profile of the ice sheet along the Marie Byrd Land traverse route, as deduced from the seismic, gravity, and altimetry observations, is shown in

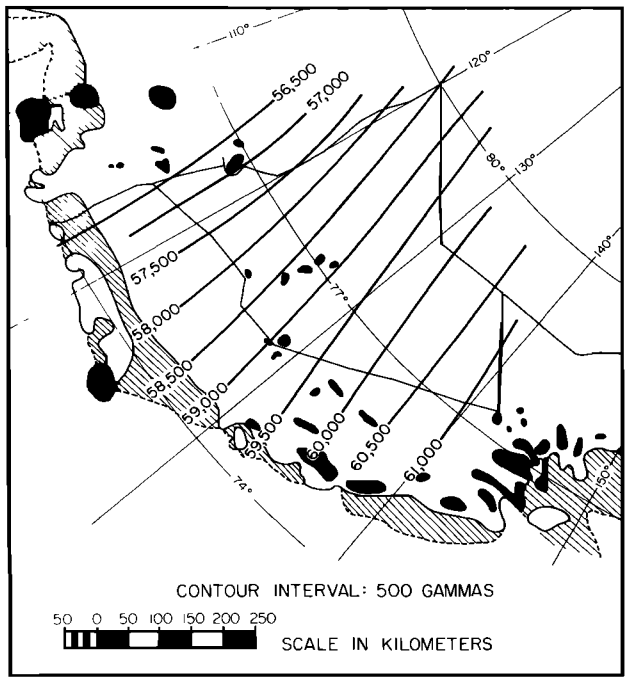

Fig. 8. Map of regional magnetic intensity.

Figure 10. As we shall see in a later section, there is good reason to believe that the land has been depressed by the load of the ice to produce approximate isostatic equilibrium. The amount of this depression has been estimated on the basis of Archimedes' principle, assuming that mantle rock of density 3.3 g/cm^3 has been displaced by ice of density 0.9 g/cm^3. Ice thickness values were averaged over a distance of 110 km along the traverse route to introduce a degree of 'regionality' into the isostatic computation; the crustal depression was then taken to be 0.27 times the mean ice thickness, reduced, in the appropriate region, by the effect of the superimposed water load that is deduced to have existed before glacierization.

The result is shown in Figure 10, the negative ordinate of the curve relative to sea level indicating the amount of depression. In this way, the same curve indicates 'adjusted sea level,' i.e. the height of the sea relative to the rock surface in the absence of ice, with no allowance for eustatic change due to melting of the ice. Any global change in sea level could easily be superimposed; it would in any event be small compared with the inferred crustal warping.

Contour maps of ice surface and subglacial topography and ice thickness (Figures 11, 12, and 13) have been prepared using the results from this and adjacent traverses [*Bentley and Ostenso*, 1961; *Thiel*, 1961; *Behrendt et al.*, 1962]. On the map of subglacial topography (Figure 12), the estimated 'adjusted shoreline,' i.e. the adjusted sea-level contour, has been drawn, thus approximating the preglacierization coastline. Allowance for a higher stand of the sea would shift this coastline only slightly in most places because of the steepness of the rock surface.

Surface Topography

In the Executive Committee Range (76.5°S, 127°W), the ice sheet surface (Figure 11) reaches an elevation of more than 2300 meters, its highest in Marie Byrd Land. The slope southwestward toward the Ross ice shelf is gentle and regular across the low-lying rock surface. A surface ridge runs westward from the Executive Committee Range into the Flood Range, reaching surprisingly near the coast at 135°W longitude. The ridge also runs eastward and then southeastward, with slowly decreasing elevation, to merge with the divide between the Amundsen Sea and Ross Sea drainage systems. Damming of the ice behind both the Crary Mountains and Toney Mountain is indicated by the sharp drop in surface elevation northward across each mountain group (Figure 10). A slight but definite decrease in elevation southward from Toney Mountain toward the Crary Mountains may be a reflection of the deep underlying subglacial trough.

On the southwestern flank of the central ridge, the mean surface slope is 4 m/km. If we assume that the average basal shear stress, $\bar{\tau}$, is given by $\bar{\tau} = \rho g \bar{\alpha} \bar{h}$, where ρ is the density of ice, g is the acceleration of gravity, $\bar{\alpha}$ is the mean ice surface slope, and $\bar{h}$ is the mean ice thickness [*Nye*, 1952], then $\bar{\tau}$ in this region ($\bar{h}$ = 1500 meters) is roughly 0.5 bar.

Northward from the central ridge, the slope is much steeper. The mean slope is 15 m/km for the first 50 km inland from the ice shelf north of Toney Mountain, and just as great between Mount Petras and the coast, where the elevation drops 2000 meters in 130 km. Along the former section, the average ice thickness is about 1000 meters, leading to a computed $\bar{\tau}$ of 1.3 bars, twice the value on the other side of the ice divide. Although the ice thickness is not known north of Mount Petras and elsewhere between the traverse route and the coast, the basal shear stress must surely reach this same average

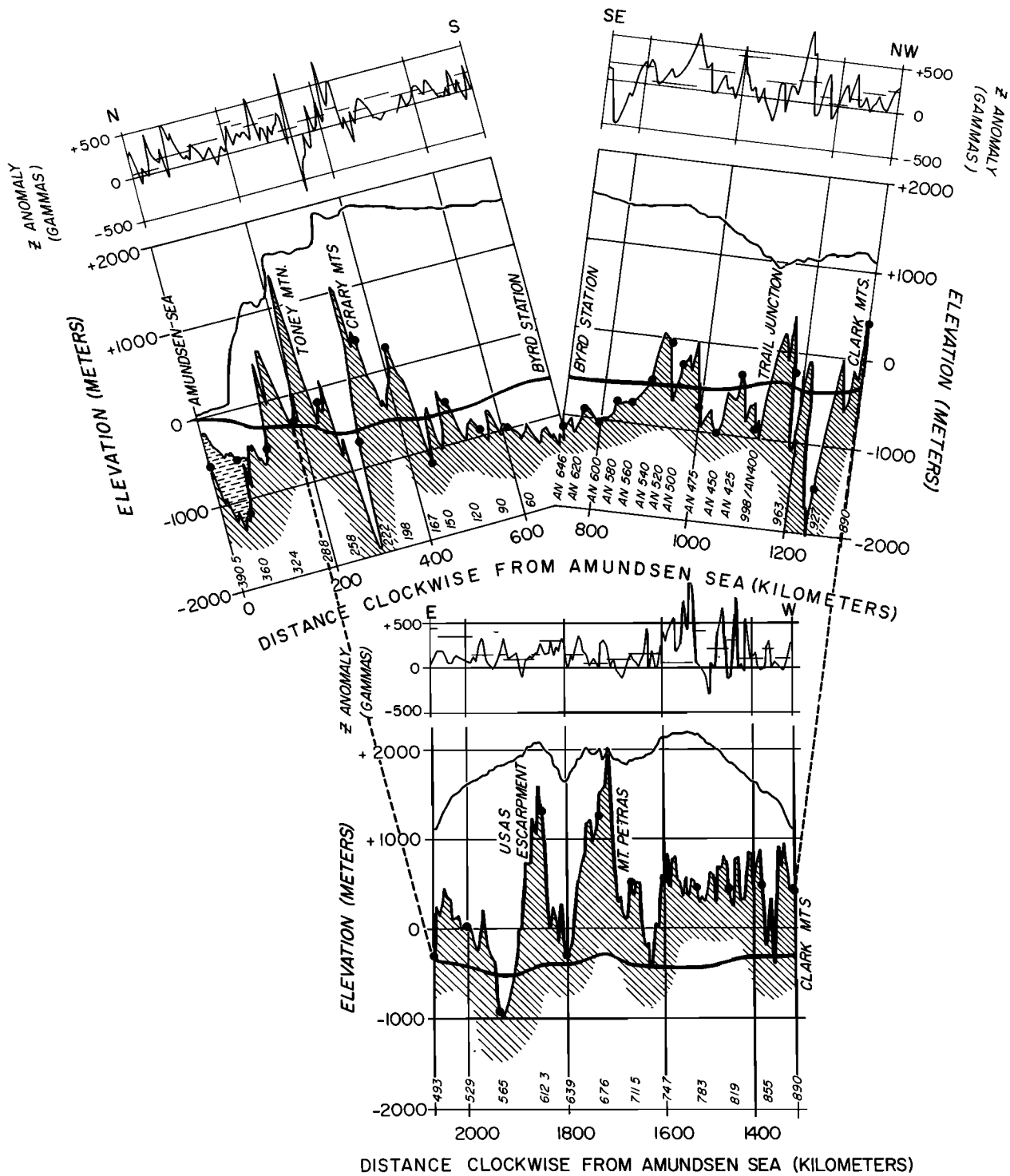

Fig. 9. Profile of ice sheet and residual vertical magnetic intensities. Byrd station is in center of upper diagram. Solid line through rock topography indicates inferred crustal depression, or 'adjusted sea level.' Horizontal line segments on magnetic profile indicate concurrent activity range at Byrd station.

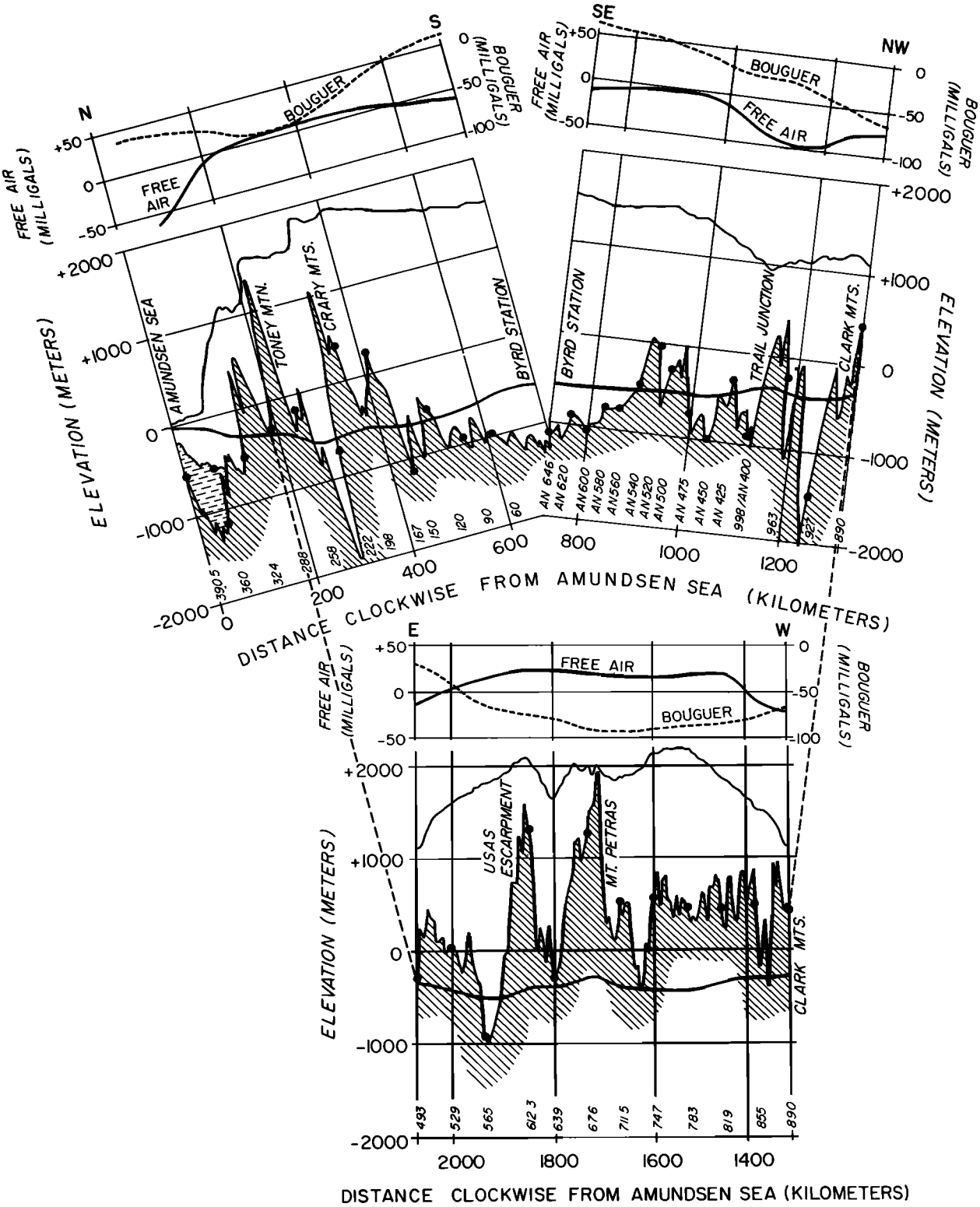

Fig. 10. Profile of ice sheet and mean gravity anomalies. Byrd station is in center of upper diagram. Scales for free-air and Bouguer anomalies are, respectively, at left and right end of each profile section. Solid line through rock topography indicates inferred crustal depression, or 'adjusted sea level.'

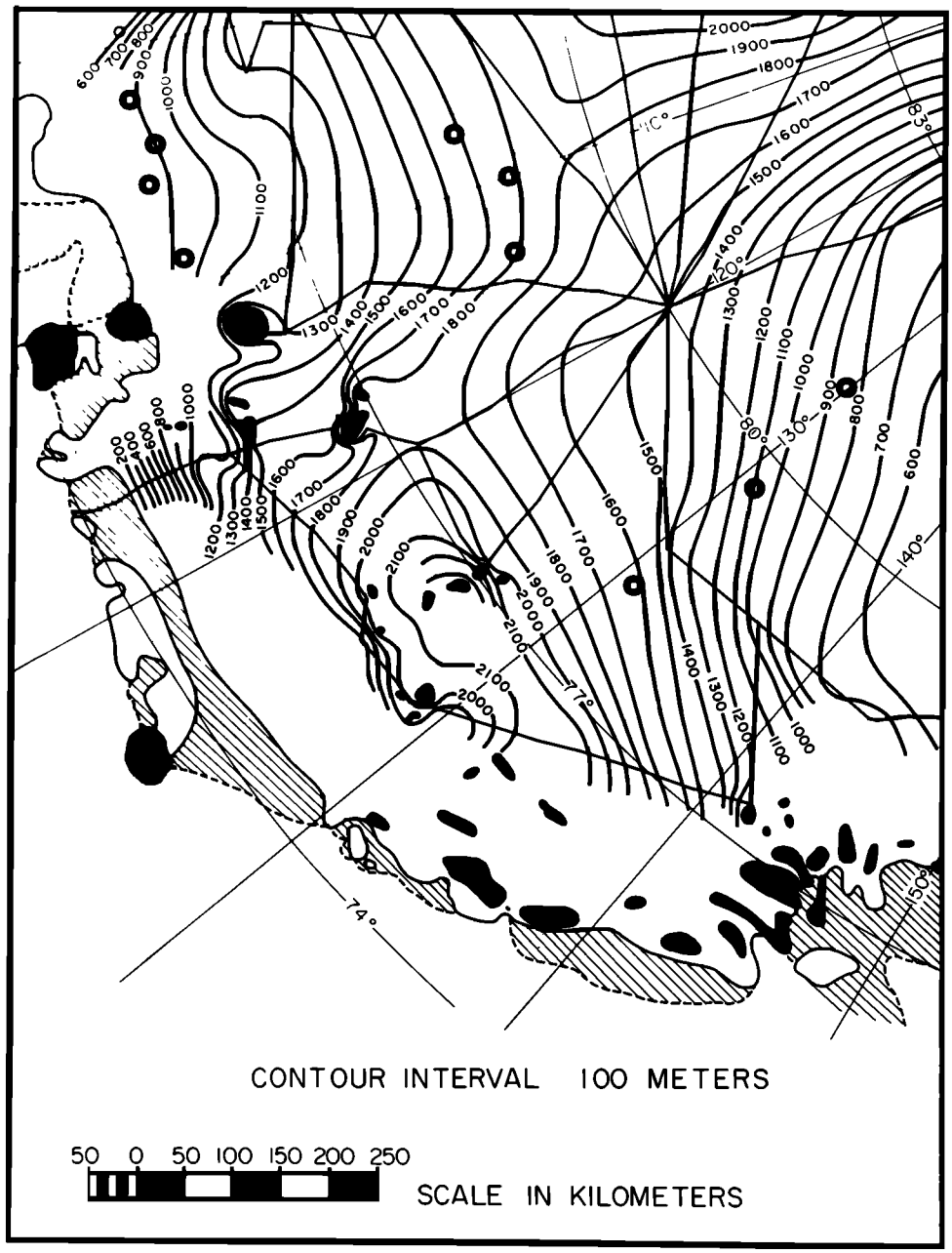

Fig. 11. Ice surface topography in Marie Byrd Land.

value over extensive regions. It appears, therefore, that the basal shear stress is roughly twice as great in the coastal areas as in the more central parts of West Antarctica.

At least part of this difference is probably due to the greater accumulation and lesser ice thickness in the coastal regions. We can obtain an estimate of the magnitude of this effect by a simple calculation. Although the mechanism of the differential horizontal motion in the ice is not certain, it can be safely assumed that most of the shearing strain takes place at or near the base of the ice [*Nye*, 1959].

It is quite sufficient for our purposes to assume that the outward velocity of the ice is uniform with depth, and that it depends upon the basal shear stress raised to some power m:

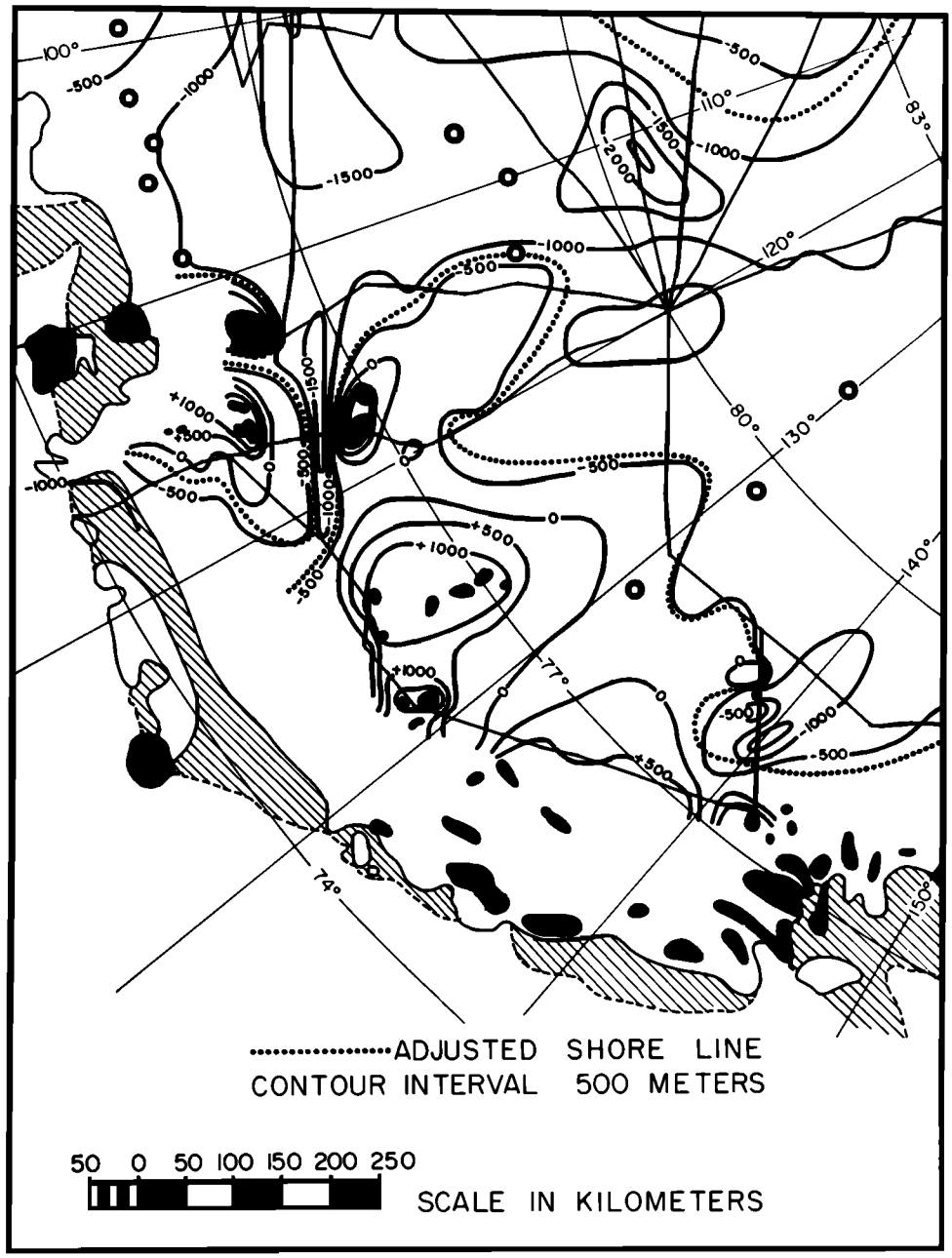

Fig. 12. Subglacial topography in Marie Byrd Land. Dotted line shows estimated position of pre-glacierization shore line.

$$v = \bar{\tau}^m$$

If steady-state flow conditions exist, i.e. the ice sheet is neither growing nor shrinking, then

$$ax = hv$$

where x is the distance from the center of the ice sheet, h is the ice thickness, and a is the ice accumulation rate, assumed to be constant in one region. Combining the two equations, we find

$$\bar{\tau} = (ax/h)^{1/m}$$

For similar values of x in the two regions, h is about twice as great in the central regions as near the coast, and a is about twice as great near the coast

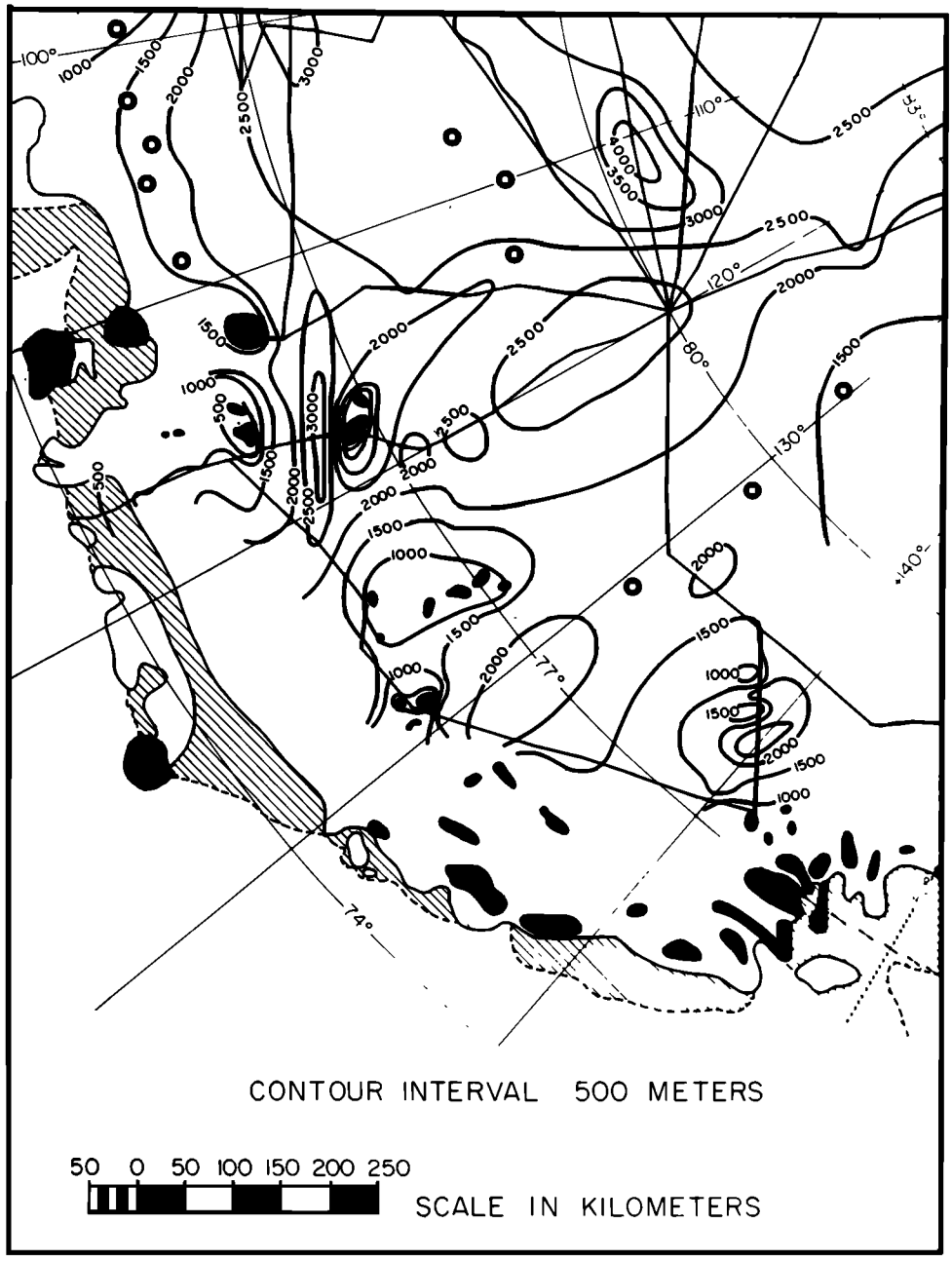

Fig. 13. Ice thickness in Marie Byrd Land.

[*Giovinetto*, 1964]; we thus find that the shear stress ratio should be $4^{1/m}$. Calculations and experiments indicate that m in all probability lies between 2 and 3 [*Glen*, 1955; *Weertman*, 1957; *Nye*, 1959], so that the stress ratio would be between 1.6 and 2, which is about the observed value. Thus these factors alone may be enough to account for the asymmetry of the Marie Byrd Land ridge.

Another factor that may be important is a difference in temperature at the base of the ice. Unfortunately, it is not possible to obtain a meaningful quantitative estimate of this factor, since both the value of the basal temperature and its effect upon the shear stress depend to a large degree upon the mechanism of differential motion, which is uncertain. Whatever the mechanism, however, we can say

that a colder temperature would tend to increase the surface slope, other things being equal. In the absence of important frictional heating in the bottom ice layers, the basal temperatures in the coastal regions would be lower, so that we can at least conclude that a temperature difference could contribute to the observed asymmetry in surface profile.

Rock Topography

The rock topography of Marie Byrd Land is extremely rugged, particularly in the eastern part. There are a number of peaks that rise several thousand meters above the level of the surrounding land. A deep trench cuts to nearly 2000 meters below sea level between the Crary Mountains and Toney Mountain, becoming shallower to the northwest and broadening into the Byrd subglacial basin to the southeast. The rock surface between the Executive Committee Range and the Crary Mountains on the south side of the trench is assumed, for the sake of mapping, to lie between present and adjusted sea level. The reason for this is that most of the rock surface beneath the traverse tracks lies above adjusted sea level, even at distances as large as 100 km from the nearest exposed rock; examination of Figures 10 and 12 shows that between the Byrd subglacial basin and the edge of the continent rock elevations below adjusted sea level are found only in the deep trench. Nevertheless, it is entirely possible that the Executive Committee Range and the Crary Mountains were separated by open water before glacierization. There is also the possibility, of course, that a high subglacial ridge connects these peaks. This is unlikely, however, because of the volcanic nature of the mountains [*Doumani and Ehlers*, 1962] and the low rock elevations elsewhere in the vicinity.

The symmetry of Mount Takahe, coupled with the rapid southward drop in subglacial rock elevation found on the 1957–1958 traverse [*Bentley and Ostenso*, 1961], makes it probable that the rock surface falls below adjusted sea level between Mount Takahe and Toney Mountain, and between Mount Takahe and Mount Murphy to the north.

A northwestward extension of the trench between Toney Mountain and the Crary Mountains is found with shallower depth beneath the north leg of the traverse. Farther to the west, subglacial spurs of the Usas escarpment and Mount Petras exhibit a relief of some 2000 meters, being separated by a valley whose floor is close to adjusted sea level.

West of Mount Petras is another valley reaching about to adjusted sea level. Still farther west, the subglacial terrain is considerably less rough, maintaining an elevation averaging 700 meters above adjusted sea level to the Clark Mountains. This relative smoothness disappears immediately to the south, where the subglacial slopes of the mountains fall to a valley cutting 1600 meters below adjusted sea level. The rough terrain continues for about 200 km to the southeast, with an average elevation near adjusted sea level before reaching the relatively smooth floor of the Byrd subglacial basin.

From the actual soundings, no matter what interpretation is applied in contouring, it is apparent that there are substantial areas of true land in Marie Byrd Land. Since there is no reason to believe that the traverse route did not cross a representative section of central Marie Byrd Land, it seems probable that before the formation of the ice sheet there was a large island extending from the Executive Committee Range or even farther east to the Edward VII Peninsula, bounded by the Byrd subglacial basin on the south. Lying off the coast of this island to the east and northeast were several smaller islands including Mount Murphy and Mount Siple, Bear Peninsula, and possibly Mount Takahe, each of which was probably a single volcanic cone. It is in the realm of speculation whether the Crary Mountains were a part of the main island or lay offshore; in either case, the associated land extended, continuously or discontinuously, for some 250 km to the southeast. Similarly, the land associated with Toney Mountain extended 100 km or so to the north and east, and might have included Mount Takahe.

The map of ice thickness (Figure 9) largely reflects the subglacial topography, since the subglacial relief is so much greater than that of the ice sheet surface. A maximum thickness of more than 3000 meters occurs in the trough between the Crary Mountains and Toney Mountain. Assuming that the traverse route represents an average sampling of the region, the mean ice thickness in Marie Byrd Land is 1770 meters.

Magnetics

The regional magnetic map (Figure 8) shows a regular increase in the vertical intensity (Z) from geographic east to west, i.e., toward the magnetic pole, as one would expect. The gradient appears slightly steeper in the eastern than in the

western part of Marie Byrd Land. The reality of this distinction is uncertain, however, in view of the errors in observation, in regional curve fitting, and in drawing the map with no more than two points on any one isomagnetic line.

With station spacing of 5½ km, it is apparent that no anomaly shapes in the profile of residual vertical intensity (Figure 12) will be well enough determined to permit valid source depth calculations, even if the subglacial and ionospheric contributions could be satisfactorily distinguished. A comparison of large anomalies with subglacial topographic variations, however, can provide a few clues to the nature of the buried geology.

The most striking anomaly is that associated with the Crary Mountains, having an apparent peak-to-peak amplitude of nearly 1400 γ. Since the feature is narrow, the apparent maxima and minima having been observed on consecutive stations, the true amplitude may be considerably larger. The large susceptibility of the subglacial rock indicated by this anomaly is supported by the analyses of *Doumani and Ehlers* [1962], who found a magnetite content of 4% to 15% in six samples of andesites, trachytes, and basalts from the Crary Mountains. A magnetite content of 10% implies a susceptibility (k) of the order of 0.05 cgs, a very high value. With this susceptibility, for example, a vertical dike 1 km high and 400 meters wide, buried under 1 km of ice, would give rise to an anomaly 1200 γ in amplitude. Thus the measured magnetite content is more than sufficient to explain the large amplitude of the anomalies associated with the Crary Mountains. The large size of the negative part of the anomaly, however, suggests an important degree of remanent magnetization with a direction of magnetization substantially different from that of the present field, which is nearly vertical (about 75° dip). Southward from the Crary Mountains, there appears to be a good qualitative correlation between the subglacial peaks near miles 167 and 120 and corresponding Z anomaly maxima, suggesting that these buried peaks are petrologically similar to the Crary Mountains.

In view of the strong magnetic effect of the Crary Mountains, it is surprising to observe the absence of any significant anomaly associated with Toney Mountain, where the exposed rocks are similar [*Doumani and Ehlers*, 1962]. Since the subglacial spur of this peak which lies beneath the traverse track rises some 1500 meters above the rock level on either side, reaching within a few hundred meters of the ice surface, the susceptibility of the rock must be much lower than that found in the Crary Mountains. Order-of-magnitude calculations indicate that the absence of an anomaly greater than a few hundred gammas implies a magnetite content of no more than a few tenths of a percent. Although *Doumani and Ehlers* [1962] reported no measurable amount of magnetite in the single sample (a trachyandesite) from Toney Mountain, the probability that a mass of rock the size of this buried spur could consist of the same basic volcanics as those of the Crary Mountains, yet be almost lacking in magnetite, is very small. The implication is strong that the subglacial peak comprises more acidic rocks than were collected from Toney Mountain, perhaps similar to the rhyolites and dacites found to the west in the Usas escarpment and Mount Petras, or perhaps a young acidic differentiate of the Toney Mountain magma. The assumption of volcanics of some kind is justified in view of the nearness of Toney Mountain and the lack of evidence that any other rock type exists in eastern Marie Byrd Land.

The buried peak with a relief of roughly 1 km north of Toney Mountain (between miles 288 and 324) also shows no associated magnetic anomaly, suggesting a composition similar to that of the Toney Mountain spur. Still farther north, there appears to be a renewed association between magnetic highs and peaks in the bedrock topography.

There are no large anomalies associated with the spurs of the Usas escarpment and Mount Petras on the northern leg of the traverse. In 18 of 19 rock samples obtained from these mountain groups, *Doumani and Ehlers* [1962] found no more than a trace of magnetite. The one exception, containing 17% magnetite, is taken from olivine basalt capping the western exposed peak of the Usas escarpment. Apparently this basalt is not present in large quantity beneath the traverse track. The rest of the rocks are rhyolitic to dacitic tuffs and flows and granodiorite.

Between Mount Petras and the Clark Mountains, the anomaly amplitudes are once again large. Some of them are associated with the subglacial topography, such as the three consecutive peaks between km 1400 and 1500, whereas some are not, for example the very large anomaly just east of station 783. On the basis of geographic proximity plus a mean rock elevation nearly 1 km above adjusted sea level, this region can be considered a southern extension of the Flood Range. The relatively low topographic

relief and the variable magnetic character suggest that this region belongs to the plutonic and metamorphic province of western Marie Byrd Land rather than to the Cenozoic volcanic province to the east.

The anomalies diminish again west of km 1400 and are low in the vicinity of the Clark Mountains, which are made up largely of granites and metasediments [*Doumani and Ehlers*, 1962] without significant magnetite content.

The profile from the Clark Mountains to Byrd station shows large anomalies that lack good correlation with the subglacial topography. The anomaly amplitudes suggest the presence of highly susceptible rocks, such as those of the Crary Mountains, but the lack of topographic correlation implies that such rocks are not the major constituents of the buried peaks. Unfortunately, there are no nearby outcrops for comparison.

The deep, broad negative anomaly near Byrd station is a peculiar feature, one that suggests a temporal change in the magnetic field rather than a geologic effect. The Byrd station record does show a decrease in vertical intensity, but it amounts to only 150 γ and occurs two hours after the minimum was recorded on the traverse profile. The anomaly, therefore, must truly reflect the buried rock. Because there is no prominent positive anomaly, despite the nearly vertical magnetic inclination, it is difficult to explain the negative anomaly without resort to remanent magnetization in a direction having a large component opposite the current field direction. This suggests the presence of a basaltic flow with reversed polarity.

Gravity

As the gravity anomaly at any individual station depends primarily on the subglacial rock elevation, some method of eliminating the effect of the topography is necessary before any other conclusions can be reached from the gravity observations. Where seismic soundings provide the ice thickness, a Bouguer anomaly can be computed, but there is no information on which to base corrections for the surrounding subglacial terrain; furthermore, the stations are very widely spaced. At most stations, no independent measurement of ice thickness at all is available, and only a free-air anomaly can be calculated. In both cases, however, averaging over many stations will tend to eliminate the effect of the terrain, since the buried terrain effect is as likely to be negative as positive. (This, of course, is not true for surface terrain effects.) Although individual gravity anomalies cannot be used for any local geological interpretation, we can hope to find meaningful regional variations from the mean anomalies.

Regional averages have been computed as part of a study of the gravity variations of West Antarctica [*Bentley*, 1968]. In this study, the map of West Antarctica has been divided into squares 111 km (1° of latitude) on a side, and the average free-air anomaly has been computed for each square. Means for squares 222 km (2°) on a side were taken as the arithmetic average of the means of the smaller squares, regardless of the number of actual observations in each 1° square, to prevent bias toward the areas with greater concentrations of gravity measurements. The total number of observed values ranged from 10 to 130 in a single 1° square, and from 40 to 200 in a single 2° square. Since the traverse routes were chosen largely without regard to the subglacial topography, we can expect this procedure to provide a reasonable mean of topographic variations too short to be isostatically compensated. One should keep in mind, however, that in some cases, notably along the northern leg of the Marie Byrd Land traverse, the 2° means comprise merely linear averages along sections of a single traverse route. It is thus possible that they may differ significantly from true areal means.

The sampling problem is much more serious for Bouguer anomalies than for free-air anomalies. The number of seismic soundings ranges from 1 to 4 per 1° square, and from 3 to 16 per 2° square. In places of irregular subglacial topography, these few soundings may be quite unrepresentative of the area as a whole. We have therefore used the additional information about ice thickness furnished by the gravity measurements by computing the mean equivalent elevation (see section *Gravity* above) from all data for each square, and then calculating the mean Bouguer anomalies from these means and the mean free-air anomalies. Although this process is in part redundant, it is justified by the fact that rock elevations are computed from relative rather than absolute free-air anomalies. The mean Bouguer anomaly in each square is, in effect, calculated from a number of *independent* measurements equal to the number of seismic soundings, and then corrected for deviations from the topographic mean.

Mean free-air anomalies in the southern part of

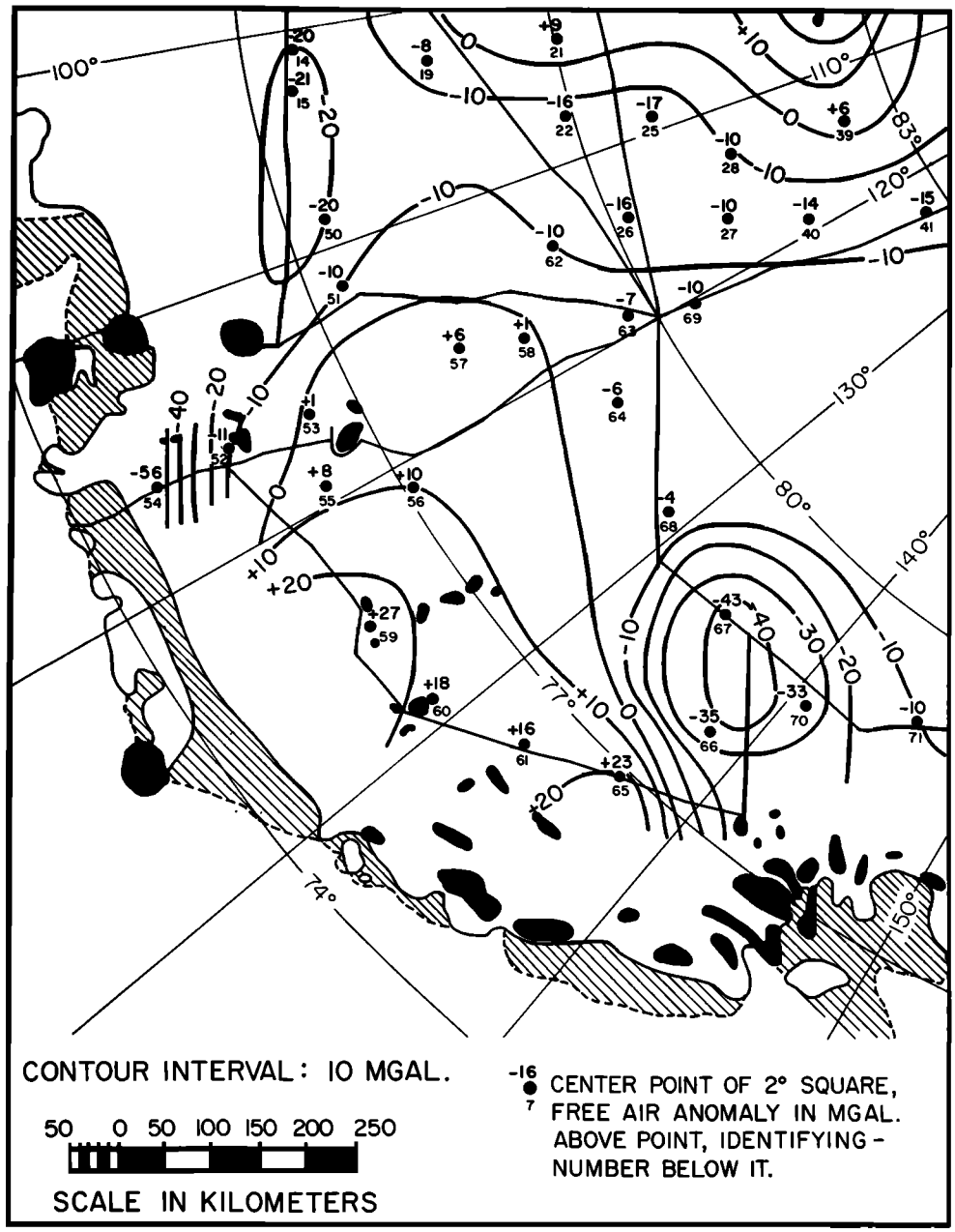

Fig. 14. Mean free-air gravity anomalies in Marie Byrd Land.

Marie Byrd Land and vicinity (Figure 14) are small. This region is bordered in eastern and western Marie Byrd Land by strong negative anomalies reaching −56 and −43 mgal, respectively, and in the north by positive anomalies up to +27 mgal. The profile along the traverse route (Figure 10) shows that these anomalies are generally associated with mean topographic variations, but that the western minimum is offset by 100 km from the associated subglacial trough. The Bouguer anomalies (Figure 15) decrease in a more or less regular fashion from +10 mgal near Byrd station to −90 mgal in the vicinity of Mount Petras and the Flood Range, with no striking anomalies.

It is well known that mean free-air anomalies over very large regions are a good approximation to mean isostatic anomalies, since the average gravitational field value depends much more on the total

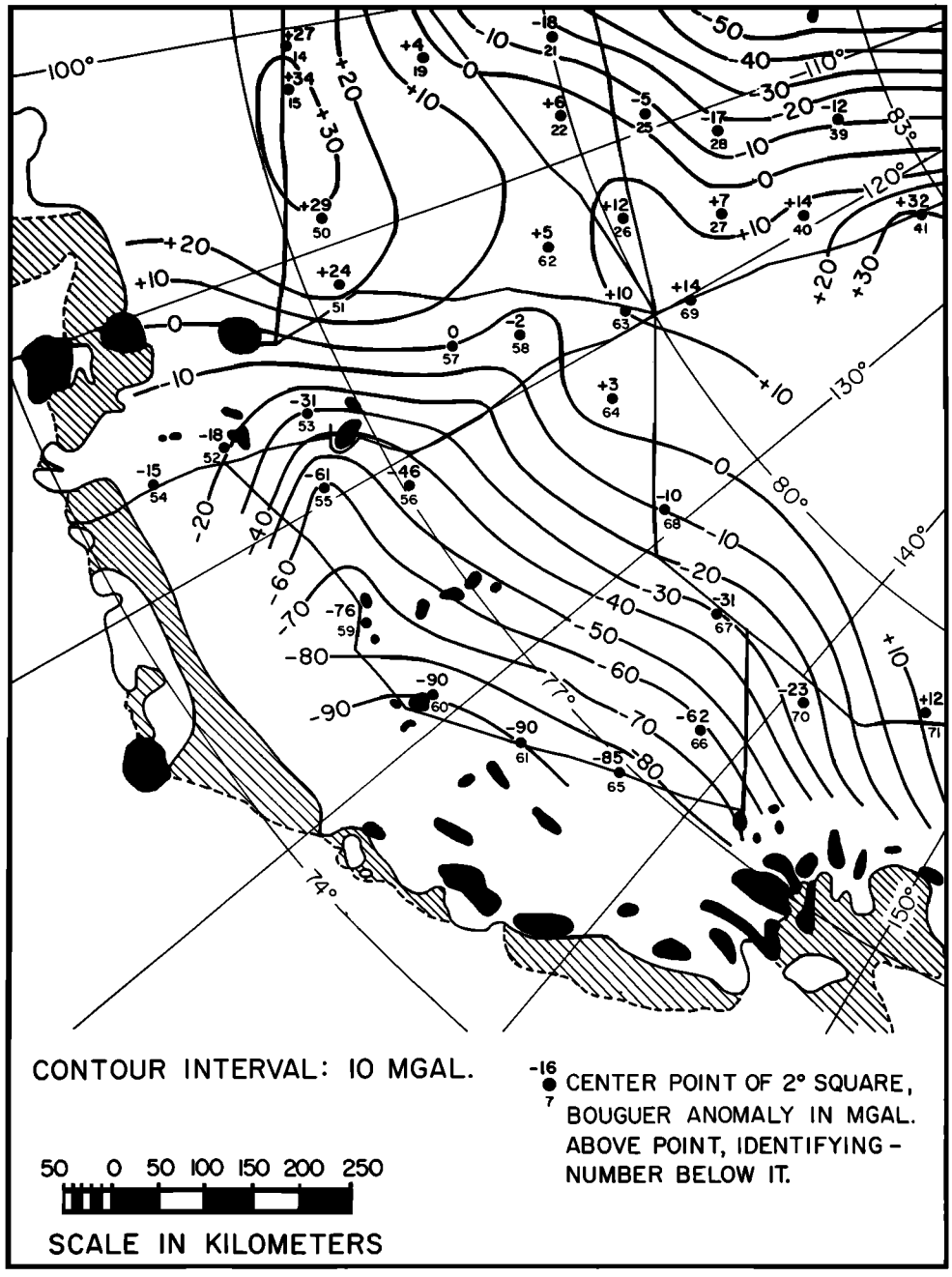

Fig. 15. Mean Bouguer anomalies in Marie Byrd Land.

mass beneath a region than on the vertical distribution of that mass. For areas 200 km in a side, however, we expect to find a correlation between mean free-air anomaly and topographic elevation, assuming isostatic balance, resulting from the finite size of the topographic and compensating masses. The gravity difference to be expected for a given topographic difference depends not only on the depth of compensation, but also on the distribution of masses in the surrounding areas. We do not, therefore, expect to find a closely defined linear regression of anomalies upon elevation, but we can expect to find a consistent trend throughout a region.

This is clearly shown in Figure 16, where we have

TABLE 2. Mean Free-Air and Bouguer Anomalies and Equivalent Elevations, Marie Byrd Land and Vicinity, Averaged over 2° Squares

2° Square Index No.	No. of 1° Squares	No. of Gravity Stations	No. of Seismic Stations	Mean Equiv. Elev., meters	Mean Free-Air Anom., mgal	Mean Bouguer Anom., mgal
14	4	114	13	−420	−20	+27
15	3	99	11	−490	−20	+34
19	3	60	8	−110	−8	+4
21	3	79	9	+240	+9	−18
22	3	85	10	−200	−16	+6
25	4	109	11	−110	−17	−5
26	4	232	16	−250	−16	+12
27	4	253	13	−180	−10	+7
28	3	121	8	+10	−10	−17
40	3	114	7	−300	−14	+14
41	2	45	3	−420	−15	+32
50	3	62	6	−440	−20	+29
51	3	63	6	−300	−10	+24
52	3	96	7	+60	−11	−18
53	3	89	8	+290	+1	−31
54	2	41	3	−370	−56	−15
55	3	95	8	+620	+8	−61
56	3	63	7	+500	+10	−46
57	3	64	6	+50	+6	0
58	4	102	10	+30	+1	−2
59	2	45	4	+920	+27	−76
60	2	46	4	+940	+15	−90
61	2	41	4	+940	+15	−90
62	3	93	10	−130	−10	+5
63	4	211	14	−150	−7	+10
64	3	60	9	−80	−6	+3
65	2	43	3	+960	+23	−85
66	3	78	6	+240	−35	−62
67	2	52	7	−110	−43	−31
68	2	30	7	+50	−4	−10
69	3	175	11	−210	−10	+14
70	3	71	6	−90	−33	−23
71	2	30	3	−200	−10	+12

plotted mean free-air anomalies for Marie Byrd Land against mean equivalent elevations. A regression line with a slope of 28 mgal/km has been fitted by least squares to values from all squares except 54, 66, 67, and 70, which are clearly anomalous. This slope is large compared with those found elsewhere [*Uotila*, 1960; *Strange and Woollard*, 1964], but is in accord with data from the rest of West Antarctica (Bentley, unpublished data). We can conclude that the observations are consistent with a state of isostatic balance within most of Marie Byrd Land.

It can further be concluded that there is over-all isostatic compensation for the ice, which produces a mean attraction of 64 mgal. The intercept of the regression line at zero equivalent elevation is −6 mgal. Although from the standpoint of internal consistency this intercept may appear to be significant, it cannot be considered as such, since the over-all mean free-air anomaly could be in error by this amount, or the mean surface elevation for the region could be in error by 20 meters.

The anomalously negative gravity values apparent in Figure 16 occur in the two areas previously noted in Figure 14. Square 54, in which the mean anomaly falls 40 mgal below the regression line,

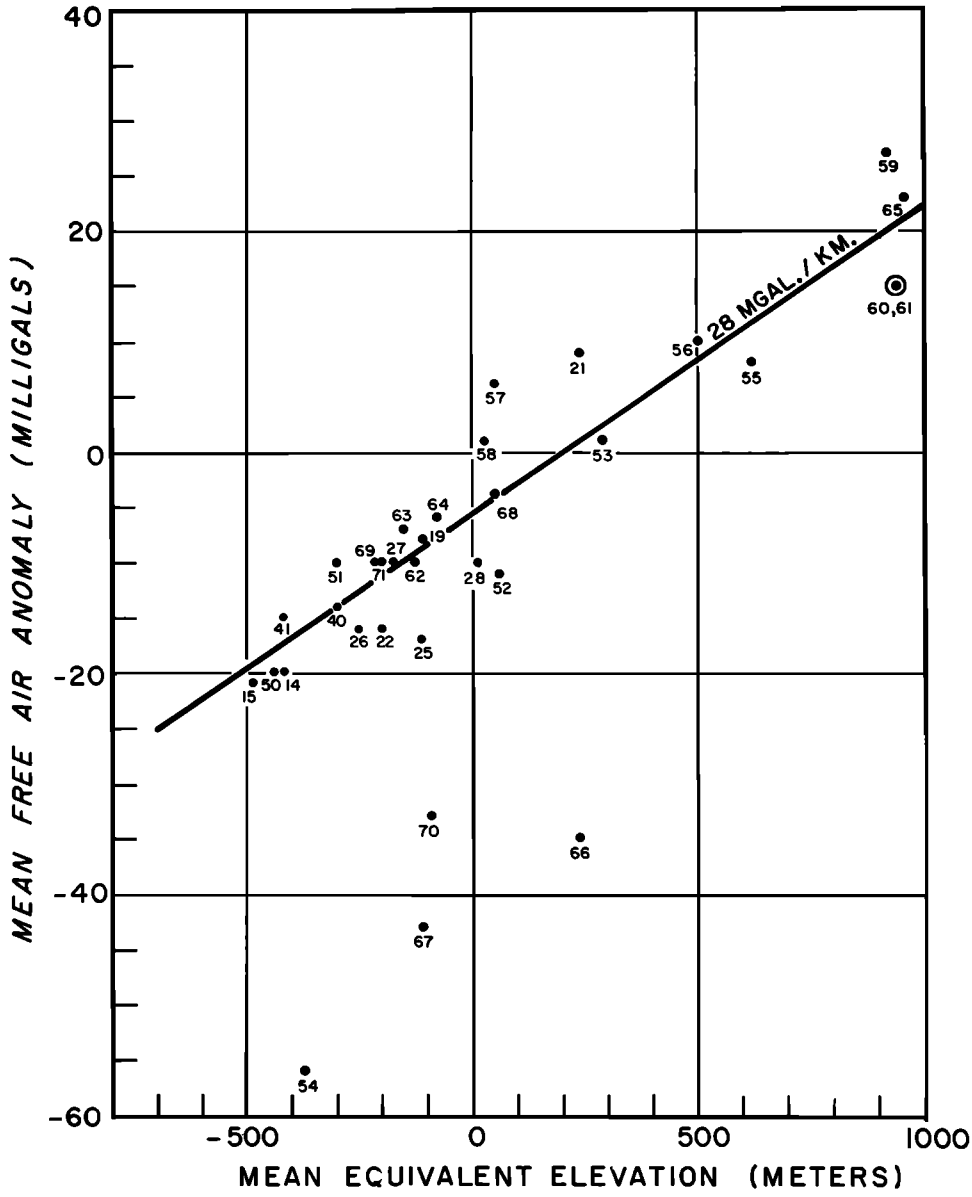

Fig. 16. Comparison of mean free-air anomaly with mean equivalent elevation.

adjoins the Amundsen Sea coast in eastern Marie Byrd Land. As a possible explanation for this low value, let us consider the effect on the gravity of a recent retreat of the ice, which would produce a large change in ice thickness near the coast.

Sample computations based on an equilibrium profile given by *Nye* [1959, p. 498], taking the central ice thickness as 2000 meters and the ice sheet half-width as decreasing from 400 to 300 km, indicate a decrease in ice thickness at the present edge of the grounded ice that would be about 1000 meters greater than that 150 km inland. This would correspond to an anomaly difference of 40 mgal, just that observed. Changing assumptions about the maximum thickness and the half-width do not substantially alter this value.

In order to explain the whole anomaly in this way, however, it would be necessary to assume that there has been essentially no isostatic rebound after load removal. This is unrealistic. The amount of crustal depression should decrease by a factor of exp $(-t/t_0)$ in t years after load removal; from measure-

ments in Fennoscandia, t_0 appears to be on the order of 5000 years [*Heiskanen and Vening Meinesz*, 1958, part 10B]. Even after only 2000 years, the gravity anomaly should have diminished by a third, and after 5500 years by two thirds. Observations by *Black and Berg* [1964] and *Bennett* [1964] suggest that the ice retreated in the Ross Sea area contemporaneously with the end of the Wisconsin (Wurm) glaciation. It is unlikely that a major retreat would have occurred much more recently in the present case.

The other abnormally low gravity values (squares 66, 67, and 70) are all found in western Marie Byrd Land. The minimum value is about 36 mgal below the regression line (equivalent, for example, to an uncompensated lowering of the rock surface by 320 meters). Since an anomaly of this numerical size and limited areal extent (Figure 14) obviously cannot be explained in terms of changing ice thickness, it appears that there are current or recently relaxed tectonic forces maintaining isostatic disequilibrium. Unfortunately, it is not possible from the current traverse coverage to define the shape of the area of deficient gravity very well. A comparison of Figures 9 and 11 does indicate, however, that the anomaly pattern may be of different orientation, as well as offset, from the associated trough.

SUMMARY

The ice surface in Marie Byrd Land is highest in the vicinity of the Executive Committee Range, whence it slopes gently toward the Ross ice shelf, and more steeply and erratically toward the Amundsen Sea. This asymmetry can be explained by the difference in accumulation rate and ice thickness in the two regions, although a variation in basal temperature may also have an effect.

The subglacial topography of the region is extremely rugged, the total relief of the rock surface exceeding 5000 meters. Before the formation of the ice sheet, there were substantial areas of true land, particularly in the west. A large island probably extended unbroken from the Executive Committee Range or Crary Mountains in the east to Edward VII Peninsula in the west, bounded on the north by open ocean and on the south by the Byrd subglacial basin. Lying off the east and northeast coast were several smaller volcanic islands.

The magnetic profiles suggest that a subglacial spur of Toney Mountain must be different in composition from the highly susceptible rock of the Crary Mountains, perhaps a young acidic differentiate of the alkaline magma which produced the exposed mountain. The Flood Range appears to belong to the plutonic and metamorphic province of the Ford Ranges rather than to the Cenozoic volcanic province to the east. Strong negative magnetic anomalies in the Crary Mountains and near Byrd station suggest the presence of remanent magnetization in a direction quite different from that of the current magnetic field.

Marie Byrd Land exhibits general isostatic compensation for the load of the ice sheet. Negative free-air anomalies near the Amundsen Sea coast are too large to be caused by a recent retreat of the ice, except in the unlikely event that the ice front has receded on the order of 100 km in the last thousand years. A region of negative isostatic anomalies in western Marie Byrd Land is associated with, but not superimposed upon, a subglacial trough cutting 2000 meters below sea level.

Acknowledgment. The authors gratefully acknowledge the assistance of the members of the field parties in collecting the field data. Particular thanks go to P. E. Parks, who not only conducted a major part of the field program, but also aided in the reduction of the gravity observations.

Contribution 190 from the Geophysical and Polar Research Center, Department of Geology, University of Wisconsin.

REFERENCES

Anderson, V. H., The petrography of some rocks from Marie Byrd Land, Antarctica, *Ohio State Univ. Res. Found. Rept. 825-2,* part 8, 27 pp., 1960.

Behrendt, J. C., T. S. Laudon, and R. J. Wold, Results of a geophysical and geological traverse from Mt. Murphy to the Hudson Mts., Antarctica, *J. Geophys. Res., 67,* 3973–3980, 1962.

Bennett, H. F., A gravity and magnetic survey of the Ross ice shelf area, Antarctica, *Univ. Wis. Geophys. and Polar Res. Ctr. Rep. 64-3,* 97 pp., 1964.

Bentley, C. R., The structure of Antarctica and its ice cover, *Research in Geophysics,* Vol. 2, *Solid Earth and Interface Phenomena,* pp. 335–389, M.I.T. Press, Cambridge, Mass., 1964.

Bentley, C. R., Gravity maps, in *Magnetic and Gravity Maps of the Antarctic, Antarctic Map Folio 9,* edited by J. C. Behrendt and C. R. Bentley, American Geographical Society, New York, 1968.

Bentley, C. R., and N. A. Ostenso, Glacial and subglacial topography of West Antarctica, *J. Glaciol., 3,* 882–911, 1961.

Black, R. F., and T. E. Berg, Glacier fluctuations recorded by patterned ground, Victoria Land, in *Antarctic Ge-*

ology, edited by R. J. Adie, pp. 107–122, Interscience, New York, 1964.

Chang, F. K., Report of seismic wave studies in northwest Marie Byrd Land, Antarctica, *Bull. Seismol. Soc. Amer. 54,* 51–65, 1964.

Crary, A. P., E. S. Robinson, H. F. Bennett, and W. W. Boyd, Jr., Glacial studies of the Ross ice shelf, Antarctica, *IGY Glaciol. Rep. 6,* 193 pp., American Geographical Society, New York, 1962.

Doumani, G. A., Volcanoes of the Executive Committee Range, Byrd Land, in *Antarctic Geology,* edited by R. J. Adie, pp. 666–675, Interscience, New York, 1964.

Doumani, G. A., and E. G. Ehlers, Petrography of rocks from mountains in Marie Byrd Land, West Antarctica, *Bull. Geol. Soc. Amer., 73,* 877–882, 1962.

Fenner, C. N., Olivine fourchites from Raymond Fosdick Mountains, Antarctica, *Bull. Geol. Soc. Amer., 49,* 367–400, 1938.

Giovinetto, M. B., The drainage systems of Antarctica: Accumulation, in *Antarctic Snow and Ice Studies, Antarctic Res. Ser.,* vol. 2, pp. 127–155, AGU, Washington, D.C., 1964.

Glen, J. W., The creep of polycrystalline ice, *Proc. Roy. Soc. London, A, 228,* 519–528, 1955.

Heiskanen, W. A., and F. A. Vening Meinesz, *The Earth and its Gravity Field,* New York, 470 pp., 1958.

Nye, J. F., A method of calculating the thickness of the ice sheets, *Nature, 169,* 529–530, 1952.

Nye, J. F., The motion of ice sheets and glaciers, *J. Glaciol., 3,* 493–507, 1959.

Ostenso, N. A., and C. R. Bentley, The problem of elevation control in Antarctica, and elevations on the Marie Byrd Land traverses, 1957–58, *IGY Glaciol. Rep. 2,* IV-1 to IV-26, American Geographical Society, New York, 1959.

Passel, C. F., Sedimentary rocks of the southern Edsel Ford Ranges, Marie Byrd Land, Antarctica, *Proc. Amer. Phil. Soc., 89,* 123–131, 1945.

Strange, W. E., and G. P. Woollard, The use of geologic and geophysical parameters in the evaluation, interpolation, and prediction of gravity, *Hawaii Inst. Geophys. Rep. HIG-64-17,* 1964.

Thiel, E. C., Antarctica, one continent or two?, *Polar Record, 10,* 335–348, 1961.

U.S. Board on Geographic Names, *Geographic Names of Antarctica,* Department of Interior, Washington, D.C., 1956.

U.S. Coast and Geodetic Survey, *Magnetograms and Hourly Values, Byrd Station, Antarctica, 1959,* Department of Commerce, Washington, D.C., 1962.

U.S. Coast and Geodetic Survey, *Magnetograms and Hourly Values, Byrd Station, Antarctica, 1960,* Department of Commerce, Washington, D.C., 1963.

Uotila, V. A., Investigations on the gravity field and shape of the earth, *Publ. Inst. Geod. Phot. Cart., 10,* Columbus, 92 pp., 1960.

Wade, F. A., The geology of the Rockefeller Mountains, King Edward VII Land, Antarctica, *Proc. Amer. Phil. Soc., 89,* 67–77, 1945.

Warner, L. A., Structure and petrography of the southern Edsel Ford Ranges, Antarctica, *Proc. Amer. Phil. Soc., 89,* 78–122, 1945.

Weertman, J., On the sliding of glaciers, *J. Glaciol., 3,* 33–38, 1957.

Woollard, G. P., and J. C. Rose, *International Gravity Measurements,* Society of Exploration Geophysicists, Tulsa, Okla., 518 pp. 1963.